

SHEAR DEFLECTION OF COMPOSITE WOOD BEAMS

A Thesis

by

THOMAS DAVID SKAGGS

Submitted to the Office of Graduate Studies of
Texas A&M University
in partial fulfillment of the requirements for the degree of

MASTER OF SCIENCE

May 1992

Major Subject: Agricultural Engineering


SHEAR DEFLECTION OF COMPOSITE WOOD BEAMS

A Thesis

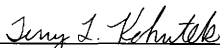
by

THOMAS DAVID SKAGGS

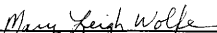
Approved as to style and content by:



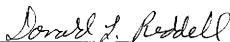
Donald A. Bender
(Chair of Committee)



Terry L. Kohutek
(Member)



Mary Leigh Wolfe
(Member)



Donald L. Reddell
(Head of Department)

May 1992

ABSTRACT

Shear Deflection of Composite Wood Beams

(May 1992)

Thomas David Skaggs, B.S., Texas A&M University

Chair of Advisory Committee: Dr. Donald A. Bender

Deflection of beams is comprised of two parts: 1) bending and 2) shear deflection. The shear component is usually ignored for most structural engineering applications; however, if the beam's construction material is lumber the shear contribution can be a significant portion of the total deflection. Calculating shear deflection for homogeneous beams is a routine mechanics of materials problem; however, when the beams are non-homogeneous, such as glued-laminated timber beams (glulam), or have non-rectangular shapes such as I-beams, it becomes more difficult to characterize deflection.

The primary objective of this research was to develop an algorithm to predict shear stress and deflection for layered composite wood beams. The shear stress model was developed using energy methods and Castigliano's theorem. The deflection model was compared to theoretical results for homogeneous beams and other published shear deflection models with close agreement being observed between the methods. The model was also compared to actual full sized glulam beam test data. Good agreement was achieved between predicted values and the actual measured values. A sensitivity analysis was performed in this research on step size for the numerical integration and on the effect of shear modulus (G) on the shear deflection.

The shear deflection model compared favorably to published models, and it has the capability of predicting shear stress in a composite beams, which is unique to this model. The advantage that this composite shear deflection model has over other published composite models is that it can calculate shear deflection for more general shapes than

previously published models. This model can calculate shear deflection for both composite glulam beams and composite I-beams. Several published models are limited to a deterministic value for G ; whereas, this model allows G to be a random variable.

ACKNOWLEDGEMENTS

I would like to give thanks to my committee chairman, Dr. Donald A. Bender, for his patience, support and guidance during this research. I would also like to thank the other members of my committee: Dr. Mary Leigh Wolfe and Dr. Terry L. Kohutck, who assisted in the completion of this thesis. I feel very fortunate to have several of the best teachers in my academic career contribute to my research.

I would like to express my appreciation to the American Institute of Timber Construction (AITC) for their technical advice. Appreciation is also extended to the Agricultural Engineering Department for financial support during this research.

Thanks should also be directed to my friends that made my years at Texas A&M University enjoyable, especially Roger Glick and the D & D Brothers, Daryl Spillmann and Derek Whitelock. These guys provided many hours of thought provoking conversation and entertainment.

Finally, I would like to thank my family. Their support and encouragement helped me in becoming a better person, instilled in me the ability to overcome hardship and gave me incentive to achieve goals that are set.

TABLE OF CONTENTS

	Page
ABSTRACT	iii
ACKNOWLEDGEMENTS	v
TABLE OF CONTENTS	vi
LIST OF TABLES	ix
LIST OF FIGURES	x
CHAPTER	
I INTRODUCTION	1
PROBLEM STATEMENT	1
RESEARCH OBJECTIVES	3
II LITERATURE REVIEW	4
PREDICTION OF SHEAR DEFLECTION	4
CHARACTERIZATION OF ELASTIC CONSTANTS	8
III MODEL DEVELOPMENT	14
SHEAR STRESS DERIVATION FOR COMPOSITE BEAMS	14
SHEAR DEFLECTION DERIVATION FOR COMPOSITE BEAMS	19
SUMMARY	21
Assumptions	21
Limitations	21
IV MODEL VERIFICATION	23
MODEL COMPARISON	23
Symmetric Two-Point Loaded Homogeneous Rectangular Beam	23
Uniformly Loaded Homogeneous Rectangular Beam	27
Homogeneous I-Beam	29
Composite I-Beam	30
Composite Glulam Beam	32

CHAPTER	Page
SUMMARY	34
V MODEL VALIDATION	36
EXPERIMENTAL PROCEDURE	36
ADJUSTMENT OF LUMBER E VALUES - METHOD 1	37
Model development	37
Test Results	38
ADJUSTMENT OF LUMBER E VALUES - METHOD 2	39
ADJUSTMENT OF LUMBER E VALUES - METHOD 3	41
SUMMARY	42
VI MODEL IMPLEMENTATION	44
EXISTING GLULAM MODEL: PROLAM	44
PROLAM Refinements	45
SENSITIVITY ANALYSES	45
Effect of Length Increment Size	45
Effect of Depth Increment Size	46
Effect of Shear Deflection	47
Effect of E/G Ratio	49
Effect of L/d on Design Equations for Deflection	50
SUMMARY	53
VII SUMMARY AND CONCLUSIONS	55
SUMMARY	55
CONCLUSIONS	57
RECOMMENDATIONS FOR FURTHER RESEARCH	58
REFERENCES	59
APPENDIX	
A COMPOSITE BEAM DEFLECTION MODEL FORTRAN CODE	63
B OROSZ'S (1970) FORM FACTOR QUATTRO PRO CODE	67
C MANSOUR AND GOPU'S (1990) FORM FACTOR FORTRAN CODE	69
D BEAM E MODEL FROM CLT MAP FORTRAN CODE	72

APPENDIX	Page
E E DATA FOR 24F-V4 GLULAM BEAMS	77
F COMPARISON OF LOCALIZED SHEAR-FREE E AND LONG- SPAN E	84
OVERVIEW OF EXPERIMENTAL DESIGN	85
TESTING EQUIPMENT	85
Two-ft Modulus of Elasticity Equipment	85
Long-Span Modulus of Elasticity Equipment	86
TESTING PROCEDURE	86
EXPERIMENTAL RESULTS	88
SUMMARY	92
VITA	93

LIST OF TABLES

	Page
Table 4.1: Results from the symmetric two-point loaded homogenous rectangular beam test scenario.	27
Table 4.2: Results from the uniformly loaded homogeneous rectangular beam test scenario.	28
Table 4.3: Results from homogeneous I-beam test scenario.	30
Table 4.4: Results from composite I-beam test scenario.	31
Table 4.5: Modulus of elasticity values assumed for the 24F-V4 glulam beam.	33
Table 4.6: Results from composite glulam beam test scenario.	34
Table 6.1: Effect of length increment on apparent modulus of elasticity.	46
Table 6.2: Effect of depth increment size on apparent modulus of elasticity.	47
Table 6.3: Effect of shear deflection model on apparent modulus of elasticity.	49
Table F.1: Comparison of localized shear-free E and long-span E - Side-A	89
Table F.2: Comparison of localized shear-free E and long-span E - Side-B	90

LIST OF FIGURES

	Page
Figure 3.1: Simple composite beam.	15
Figure 3.2: Stresses, forces and moments on the composite cross section.	17
Figure 4.1: Shear and moment diagrams for a homogeneous beam.	24
Figure 4.2: Cross sectional dimensions of a commercially produced wood I-beam.	29
Figure 4.3: 16 lamination 24F-V4 glulam beam layup.	32
Figure 5.1: Predicted E versus measured E for 24F-V4 Douglas-fir beams ($E/G = 16$).	38
Figure 5.2: Predicted E versus measured E for 24F-V4 Douglas-fir beams ($E/G = 20$ for all laminations except L3 where $E/G = 30$).	39
Figure 5.3: Empirical cumulative distribution function for various case scenarios.	42
Figure 6.1: Comparison between different shear prediction methods.	48
Figure 6.2: Effect of different E/G ratios on apparent E	50
Figure 6.3: Error in predicted deflections for different L/d ratios for a two-point symmetric load.	52
Figure 6.4: Error in predicted deflections for different L/d ratios for a uniform load.	52
Figure 6.5: Error in predicted deflections for different L/d ratios for a concentrated load at midspan.	53
Figure F.1: E_s versus E_{1s} test data.	91

CHAPTER I

INTRODUCTION

PROBLEM STATEMENT

There can be many limit states of a structural design, but one of the most important is deflection. For example, if a door header has excessive deflection the door will not shut properly. Floor systems are another design controlled by deflection. A floor with excessive deflection can cause discomfort by having a "bouncy feeling"; thus, users may lose confidence in the design. Similarly, a design that is sensitive to deflection, but is often used in the construction industry, is flat roofs. Accumulation of water can occur on flat roof systems, causing deflection due to the weight of the water, which leads to even more ponding. This is commonly referred to as the "P-delta" effect. In these types of designs, the deflection can be attributed to beams, which are the most common structural member.

Deflection of beams is comprised of two parts: 1) bending and 2) shear deflection. Shear deflection is ignored in many structural engineering applications. This is a reasonable assumption for steel structures because the total deflection is usually dominated by the bending component, except for very short, deep beams. The U.S. engineering practice accounts for shear deflection of wood members in a more subtle fashion. The expected deflection is commonly calculated using equations that only take bending into account. Design values for (E) in the National Design Specification (NDS) (1986) are reduced by about 3.4%, according to American Society for Testing and Materials (ASTM) D 245 (1991b) and ASTM D 2915 (1991c), to indirectly account for shear deflections within span-to-depth (L/d) ratios of 15 to 25. The Commission of the European Communities in Eurocode 5 (1987), as cited by Chui (1991), approach this problem in a more direct

References in this thesis follow the format established in Wood and Fiber Science.

manner. The true bending E is published as the design E , and the code specifies that shear deflection must be included in the total deflection prediction.

Shear deflection is related to the shear modulus (G) of the beam, which can also be referred to as modulus of rigidity. The relationship of E and G for a homogeneous, isotropic material is given by Gere and Timoshenko (1984) as follows:

$$G = \frac{E}{2(1+\nu)} \quad (1.1)$$

where:

- G = shear modulus,
- E = modulus of elasticity and
- ν = Poisson's Ratio.

Poisson's Ratio for steel is assumed to be 0.3 in the elastic range (Salmon and Johnson, 1990). This yields a ratio of E/G of 2.6; however, the ratio of E/G for wood is generally assumed to range from 11 to 16 (USDA, 1987). It should be noted that Equation 1.1 is invalid for wood because of its orthotropic characteristics. This characteristic explains why there is such a large discrepancy between the E/G ratio of steel and wood. This large ratio for wood indicates the shear component of the total deflection can be more significant for a wood beam than for a steel beam. Hence, shear deflection should be accounted for in certain situations.

The current practice for calculating deflection of wood beams is to use flexural equations found in many textbooks. These equations are derived for bending only, but since the design E is reduced to account for shear deflection, they give reasonably accurate predictions for L/d ratios ranging from 15 to 25. However, if the L/d ratio is less than 15, the predicted deflection will be less than the actual deflection. Modified equations can be used (Hoyle and Woeste, 1989) that take shear deflection into account; however, they are valid only for homogeneous materials.

Simple methods of predicting shear stress and deflection are needed for composite layered wood beams. The finite element approach is effective for predicting shear in beams; however, it is computationally intensive and requires detailed material property data for each element, or cell. Transformed section approaches have been developed for layered beams with homogeneous laminations; however, these methods do not fully account for lengthwise variability of the lamination elastic properties. A general, versatile method is needed to predict shear in beams for the purposes of evaluating design procedures and assessing the need for research on localized elastic properties of wood (particularly shear modulus).

RESEARCH OBJECTIVES

The specific objectives of this research are:

1. Develop an algorithm to predict shear stress and deflection for layered composite wood beams.
2. Compare the shear deflection algorithm with published methods. Comparisons will be made under the assumptions of homogeneous beams, and layered beams with homogenous properties within each lamination.
3. Experimentally validate the shear deflection algorithm using test data on glulam beams.
4. Integrate the shear deflection algorithm into an existing glued-laminated timber beam (glulam) model (Hernandez, 1991) and perform sensitivity analyses on parameters such as E/G ratios, step size for numerical integration, and beam layups.
5. Compare shear deflection predictions from the algorithm with those using approximate methods recommended for design purposes.

CHAPTER II

LITERATURE REVIEW

PREDICTION OF SHEAR DEFLECTION

Many mechanics of materials textbooks address the deflection of homogeneous beams with rectangular shaped cross sections. However, cross sections with irregular shapes or containing nonhomogeneous materials are often "beyond the scope of the textbook". The basis for many of the deflection equations for homogeneous materials are energy methods. The strain energy due to bending and shear can be found in several textbooks (e.g. Boresi and Sidebottom, 1985) as follows:

$$U = \iiint \left(\frac{1}{2E} (\sigma_{xx})^2 + \frac{1}{2G} (\tau)^2 \right) dV \quad (2.1)$$

where:

- U = internal energy of the stressed volume,
- E = modulus of elasticity,
- σ_{xx} = bending stress at any point in the beam,
- G = shear modulus and
- τ = shear stress at any point in the beam.

Castigliano's theorem, shown in Equation 2.2, then can be applied to Equation 2.1 to find the deflection of the member. This also is a common mechanics problem covered by many textbooks such as Boresi and Sidebottom (1985).

$$\delta_i = \frac{\partial U}{\partial F_i} \quad (2.2)$$

where:

- δ_i = deflection at point i and
- F_i = concentrated load located at point i .

To find deflection, Equation 2.1 is integrated across the width and depth, and the partial derivatives are taken with respect to F_i . Equation 2.3 (Boresi and Sidebottom, 1985) represents the final form after these operations have been performed.

$$\delta_i = \int_0^L \frac{M}{EI} \frac{\partial M}{\partial F_i} dx + \int_0^L \frac{kV}{GA} \frac{\partial V}{\partial F_i} dx \quad (2.3)$$

where:

- M = bending moment as a function of x ,
- I = moment of inertia,
- k = form factor as a function of beam geometry,
- V = shear as a function of x and
- A = area of the cross section.

The two terms, k and A , result from algebraic cancellations. The k factor values can be derived for different cross sections. For a rectangular cross section, k equals 1.20, and for I-beams, k is approximated as 1.00; however, only the area of the I-beam's web is used for A (Boresi and Sidebottom, 1985). This general method to calculate deflection has a large range of applications; however, it is limited to homogeneous materials.

Wangaard (1964) studied the elastic deflection of small-scale composite beams. These composite beams were 1" x 1" x 16" with wood cores that were 90% of the inner portion of the cross section. The wood cores were covered with fiberglass reinforced plastic faces on the outermost fibers, about the axis of bending. The first model examined by Wangaard predicted deflection using the usual elastic formulas that are derived from the first term of Equation 2.3 which only accounts for bending. The transformed section method (see Gere and Timoshenko, 1984) was used to calculate E , and it was found to under-predict deflection in all cases. The second model included the second term of Equation 2.3 which accounts for shear deflection. This model used G of the wood core, k equal to 1.00 and the average of the gross (wood and fiberglass) cross sectional area and the wood core area for A . The accuracy of this model was increased by including the shear term. This method is limited to cross sections that are symmetric about the neutral

axis, referred to as balanced layups, and ignores the variability of material properties (E and G) along the length of the beam.

Biblis (1965) examined the deflection of small scale solid wood beams of varying span-to-depth (L/d) ratios. Several wood species were studied for the 0.65" x 0.65" test specimens. An equation was used that could be derived from Equation 2.3 to predict deflection for simply supported homogeneous beams with k equal to 1.20. This method is limited to homogeneous simply supported beams. An important finding was the shear component could account for over 40% of the total deflection at a L/d ratio of 8 for Douglas-fir lumber. This is significant because this species grouping is commonly used in glulam beams.

Orosz (1970) used energy methods to calculate shear deflection of wood beams. He reduced the second integral in Equation 2.3 to multiplication of the area of the shear diagram with the ordinate of the desired point of shear deflection. It was also noted that k changes as the shape of the beam changes. The form factor (k) was derived for an I-beam with the flange and webs having different lumber properties. It can be applied to glulam beams, but is limited to a cross section that is symmetric about the neutral axis, and only allows two different lumber grades. A possible extension of this method would be to derive a k factor for a multi-layer composite beam that has different wood properties; however, this would be mathematically complex for a general multi-layered beam, would still be limited to balanced layups, and would ignore variability of the material properties along the length of the beam.

Mansour and Gopu (1990) presented a method to predict the deflection of long-span pitch-cambered glulam beams, using Equation 2.3 with a transformed section analysis. They presented a method to calculate k for unbalanced layered beams. Monte Carlo simulation was performed to randomly assign E values along the length and depth of the beam; however, the variation of E/G was ignored, and was limited to 16. The simulated beam was then analyzed using a finite element method. They concluded that simple equations

for homogeneous beams provide a good prediction of total deflection as long as the shear component was taken into account. This is significant since simple deflection equations used in design ignore E variability.

Swift and Heller (1974) present a Quasi-Newton method to predict deflection and shear stress distribution in layered beams. Their method analyzed glulam beams with different percentages of high quality wood ($E = 1.8 \times 10^6$ psi) and low quality wood ($E = 0.8 \times 10^6$ psi). They noted that a large portion of weaker wood in the cross section caused the shear deflection to predominate for short beams. Their method would allow for unbalanced layups; however, it would not allow for variation along the length of the laminates.

Baird and Ozelton (1984) used the shear portion of Equation 2.3 with a factor to account for tapered glulam beams, and presented a method to approximate k for different shapes, such as I-beams. They suggested a simplified approximate approach for calculating the deflection of I-beams that defines the A term in Equation 2.3 to be equal to the area of the web, and the form factor equal to unity. They also presented a simplified version of Equation 2.3, which they reduced to tabular form for solid sawn lumber. Although these tables are adequate for solid sawn lumber, they are not applicable to composite cross sections.

Since composite cross sections often utilize the stiffer materials on the outer portion of the cross section and the less stiff materials for the core, it is intuitive to use the method of transformed sections to calculate the bending stresses and deflections. Hilson et al. (1990, 1988) and Pellicane and Hilson (1985) applied this method to calculating shear deflection. They presented a finite difference equation that accounts for bending and shear as follows:

$$\delta_A = \sum_{i=1}^n \left[\left(\frac{M_i m_i}{EI_i} + \frac{k V_i v_i}{GA_i} \right) \Delta x \right] \quad (2.4)$$

where:

- δ_A = total bending and shear deflection at A ,
- M_i = bending moment at i ,
- m_i = bending moment at i due to unit load at A ,
- V_i = shear force at i ,
- v_i = shear force at i due to unit load at A ,
- EI_i = bending properties of transformed section at i ,
- GA_i = shear properties of transformed section at i ,
- k = form factor taken as 1.20,
- Δx = finite interval between sections in each element and
- n = number of longitudinal elements.

This equation is similar to Equation 2.3 with the integrals being replaced by summations, and the partial derivatives being replaced by m_i and v_i , which are the bending moment and shear force, respectively, from a unit load applied at midspan. However, this equation is not exact for composite cross sections with varying E because it does not account for the changes in the shear stresses across the various laminations. They suggested using the transformed area of the cross section with the k factor equal to 1.20 for a rectangular cross section, but these two terms are based on the assumption of a rectangular cross section, not a transformed non-rectangular cross section.

CHARACTERIZATION OF ELASTIC CONSTANTS

Being able to predict the behavior of wood under various loads is an important task. Gaining a better understanding of its characteristics could influence designers to use this material for more complex structures. Many models can predict the theoretical stresses and strains of wood systems, but these models require input in the form of elastic constants that are not completely characterized for every wood species grouping. The easiest property to obtain and the most studied is E . The next most studied is G and the

last, and probably least studied would be the Poisson's ratios (ν) about the three principal planes of the wood. These principal axes are referred to as longitudinal (L), radial (R) and tangential (T) (see Bodig and Jayne, 1982).

Some earlier work on the relationships of E and G was done by Doyle and Markwardt (1966). They tested full sized southern pine dimension lumber for a variety of structural grades. Modulus of elasticity was measured flatwise in bending and G was measured using a torsional technique. They regressed E and G and showed that the coefficient of correlation (r) varied from -0.342 to $+0.228$ depending on the lumber grade, and the E/G ratios ranged from 8.1 to 13.4 with the average being 11.6. Doyle and Markwardt (1967) followed this study with another series of tests for southern pine dimension lumber. The E was measured in tension and G again was measured in torsion. The results from these tests were similar to their previous test results. The r values for E versus G ranged from -0.147 to $+0.554$, and the E/G ratio ranged from 11.1 to 15.1 with an average of 12.8. They stated that G appeared to be less affected by grade or quality of the material than E . Doyle (1968) tested another sample of No. 2 dense kiln-dried southern pine dimension lumber. He observed that G did not correlate with flatwise E for his series of tests and the average E/G ratio was recorded as 13.5. These three studies helped determine the E/G ratio of 12 for southern pine lumber, published in the Wood Handbook (USDA, 1987); however the poor r values suggest that a deterministic number may not best represent the E/G ratio.

Palka and Barrett (1985) presented a report to the ASTM task group investigating the validity of Table 2 in ASTM D 2915-74. This testing consisted of a sample of Canadian Spruce 2" x 4" and 2" x 8" structural lumber specimens. The test was performed under third point bending with the lumber being loaded edge-wise. The total deflection at midspan and deflection relative to load heads were measured giving an indication of gross- E , with shear deflection included, and true- E , without shear deflection, respectively. The true- E/G ratio can be determined from the two E values. They stated that there was a large amount of variability in the true- E/G ratio for the two samples and that the

average value was considerably larger than the reported value of true- E/G of 16. They concluded that true- E/G is dependent on the test method and lumber quality. The table that instigated this investigation has since been replaced by a footnote (ASTM, 1991c) that states, "Limited data indicate that the E/G ratio for individual pieces of lumber can vary significantly from $E/G = 16$ depending on the number, size and location of knots present, the slope of grain in the piece and the span over which deflections are measured."

Gunnerson, et al. (1973) subjected flat plates to a two-way bending moment, caused by a triangular load configuration. They found they could simplify the calculations of E by reducing the flat plate to an equivalent simple beam with point loads; however, correction factors were required to take into account the two-way bending moment. It was concluded that the plate testing method is a good procedure for determining elastic parameters of wood. The disadvantage of this procedure is that the plates are time consuming to prepare. This method works best for plywood, particleboard and fiberboard, but is ill-suited for structural lumber.

Bodig and Goodman (1973) used plate bending and plate twisting tests on small scale clear wood specimens to predict the elastic constants of the wood. These specimens consisted of several softwood and hardwood species. The plates were manufactured to 0.3" x 6.5" x 12.5" with six different plate orientations (LR , RL , LT , TL , TR , RT) to measure E and ν about the different axes. The plates were then cut down to the dimensions 0.3 x 6.5" x 6.5" to measure G by a plate twisting test. The authors developed power-type regression equations that related the elastic constants from their results. They found a significant differences between the regression lines for softwood and hardwood species. In addition to the elastic parameters, they correlated the elastic constants to the density of the material. This resulted in a coefficient of variation on the order of 20 percent for the elastic properties versus density regressions. Power curves were statistically significant for most of the relationships; however, the regression was not significant for G_{LR} versus E_L and G_{LT} versus E_L for the softwood species. This study highlights the problem of trying to predict G by using E . Their study showed that

predicting G and E independently using specific gravity yielded r values for the regressions with statistical significance, indicating that E/G is not a constant and should be treated as two independent stochastic variables.

Goodman and Bodig (1978) presented a review of literature and a commentary on the problem of modeling elastic behaviors of wood. They commented on the problem of modeling knots and associated grain deviations. Much of the data used to characterize the elastic parameters of wood are collected from clearwood specimens; however, knots cause the analysis to become exceedingly complex. The grain deviations around the knots cause the principle axes (L, R and T) to be rotated, thus making the modeling procedure very difficult. It was concluded that compression along the ring and grain of wood (ie. knots and grain deviations) is not completely understood and further refinements of theory are needed. They also theorized that the assumptions of orthotropic symmetry in the radial direction is most often the cause for deviation between theoretical and experimental measurements. They suggested that a possible method to model lumber is an orthotropic finite element model; however, the tensor transformations for grain deviations and knots may not be a valid technique.

Ebrahimi and Sliker (1981) measured G in small scale specimens in tension. The specimens were 0.25" x 4" x 32", and were instrumented with a strain gage rosette that consisted of free-filament strain gages. These gages had to be specially fabricated because errors caused by reinforcing occur when measuring materials having an E less than one million psi, as in wood at large angles to the grain direction. Most of the stiffness of commercial strain gages comes from the plastic or paper backing instead of the strain sensitive wire or foil. The individual strain gages were oriented 45 degrees apart and the angle of grain to angle of applied stress varied between 20, 35, 50 and 65 degrees. The G values recorded from the tensile specimens were compared to flat plates 0.5" x 14" x 14" prepared according to the procedure outlined in ASTM D 3044-76 (1991d), Standard Test Method for Shear Modulus of Plywood. Shear moduli varied within $\pm 10\%$ of the G measured from the plate test at a load to grain angle of 20 degrees. The advantage of

this test method is that the specimens can be removed from structural lumber and are relatively easy to fabricate, as compared to plate testing. The disadvantages of this test method are: having to "hand-make" the strain gage rosettes, orienting the grain angle of the specimen when it is fabricated and limiting specimens to clearwood and straight-grained.

Zhang and Sliker (1991) tested small scale specimens in tension and compression to measure G and compared them to the G measured from plate testing in accordance with ASTM D 3044-76 (1991d). Two sets of off-axis specimens were used, with one set for loading in tension and the other in compression. The tension specimens were 0.5" x 1.25" x 11" and the compression specimens were 1.25" x 1.25" x 7". Free-filament strain gages were manufactured manually and were placed in rosettes as described previously (Ebrahimi and Sliker, 1981). The load to grain angles for both specimens were 0, 10, 20 and 45 degrees. The tension specimens compared more closely to the flat plate testing than the compression specimens, because the compression load heads induced shear distortion. They also confirmed Ebrahimi and Sliker's (1981) earlier finding that the best prediction of G in tension was at a load to grain angle of between 20 and 30 degrees. This method, although promising, is limited to straight-grained woods.

Davalos et al. (1991) computed G from a torsional test for small scale southern pine glulam beams. Shear modulus was measured about two planes, G_{LR} and G_{LT} , and a difference between the mean values of approximately 7 percent was found. They stated that this is statistically significant, but it can probably be ignored in practical engineering applications; therefore, can be modeled as transverse isotropic. They then compared Saint-Venant's solution for homogeneous, elastic, isotropic, rectangular sections to Navier's solution for isotropic circular cylinders (Hsu, 1984). The rectangular sections were 1.0" x 1.0", 1" x 0.5", 1.5" x 0.5" and 2.0" x 0.5" and the circular sections had a diameter of 1.0". The different depth-to-width ratios of the rectangular cross sections had no effect on the computed G . These values were close to the G values computed from the circular cross section. These findings simplify the measurement of G , because

specimens do not have to be removed from a piece of structural lumber with a certain grain orientation. Their findings also simplify the modeling of composite wood beams by suggesting that G_{LR} is equivalent to G_{LT} . This allows a composite beam to be modeled with respect to G without regard to the orientation of the growth rings.

Bradtmueller et al. (1991) subjected oriented strandboard (OSB) to a quarter-point and five-point loading schemes. These samples of OSB had thicknesses of 3/8", 23/32" and 1-1/8". The quarter-point loaded beams had two linear variable differential transducers (LVDT) located at midspan. One LVDT measured the deflection relative to the load head, and the other measured total midspan deflection. The five-point loaded beam had 3 reactions and two load heads placed symmetrically along the length of the beam. Two LVDTs were located adjacent to the load heads to measure deflection of that section of the beam. Using the deflections from both testing apparatuses, E and G could be solved for simultaneously. The sensitivity of the different parameters was analyzed and an important finding was that a small error in calculating E magnified the error in G . This is caused by E being considerably larger than G ; therefore, causing the equations to be slightly ill-conditioned. They also found that these measurements were sensitive to dimension measurements especially depth and span. They noted that experimental results of G were lower than expected and theorized that this was caused by the low shear stiffness in the core which corresponded to the highest shear stresses.

Chui (1991) used a vibration technique to simultaneously evaluate E and G . His findings revealed that the common assumption of E/G equal to 16 for Douglas-fir (USDA, 1987) may not be valid. Chui's data indicated E/G is a random variable, not a deterministic value; furthermore, it was suggested to use E/G of 20 for clearwood and 30 for lower quality lumber that contains knots. This is meaningful since the beam combinations found in the American Institute of Timber Construction (AITC) 117 - Manufacturing (1988) often specify that 50% of the inner core of glulam beams can be made with low quality lumber.

CHAPTER III

MODEL DEVELOPMENT

The use of composite beams such as glulam and I-beams with lower quality wood in their cores and webs, respectively, have made the problem of calculating deflections due to shear more complex. Varying E and G across the cross section and along the length for multi-layered beams increases the difficulty of calculating shear deformation. Researchers (Mansour and Gopu, 1990, and Orosz, 1970) have presented methods to calculate k for composite beams, for use in the traditional shear deflection equation (Equation 2.3); however, a more versatile method is needed to facilitate studies of spatial variation of E and G .

SHEAR STRESS DERIVATION FOR COMPOSITE BEAMS

An intuitive start to deriving an equation for shear deflection that considers a composite cross section would be to critically examine Equation 2.3; however, only the second term of this equation needs to be modified. The derivation of Equation 2.3 assumes the shear stress is equal to the classic shear stress used in many applications. This equation can be found in Gere and Timoshenko (1984).

$$\tau = \frac{VQ}{Ib} \quad (3.1)$$

where:

- τ = shear stress at any point in the cross section,
- V = shear force,
- Q = first moment of the area,
- I = moment of inertia and
- b = base of the cross section.

Although, this simple equation is not directly applicable to layered beams, the theory of deriving Equation 3.1 can be extended to layered beams. Finding the shear stress distribution in a homogeneous beam is straightforward; however, as material properties vary, as in a composite beam, so do the shear stress distributions. Once the shear stresses are derived for a relatively simple composite beam, it is an easy extension to cover more complex composite beams, such as glued-laminated timber beams (glulam) or I-beams. Finally, after the shear stress distribution is characterized for a composite beam, shear deflection can be found by applying the theory of complementary virtual work.

Figure 3.1(a) illustrates a simple composite beam that is stressed by arbitrary loads P , Q and w . Figure 3.1(b) represents the cross section of this beam with width b and height h . The outer laminations of this composite beam have modulus of elasticity of E_1 and the inner laminations have modulus of elasticity of E_2 . It is assumed that E_1 is greater than E_2 , an assumption that would be generally true for glulam beams. Composite beams are often analyzed using the transformed-section method, because the usual elastic beam formulas can be used with slight modification. Figure 3.1(c) illustrates the transformed cross section.

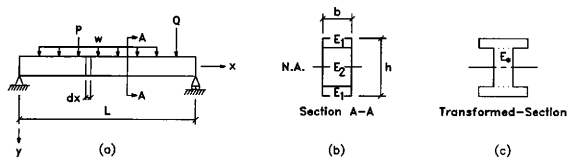


Figure 3.1: Simple composite beam.

This method transforms the composite cross section to a homogeneous material with a modulus of elasticity of E_* , where E_* is an arbitrary constant. The width of the i^{th}

lamination is adjusted by the ratio of its corresponding E_i to the constant E_* . Equation 3.2 demonstrates this transformation.

$$b_{Ai} = \frac{E_i}{E_*} b_i \quad (3.2)$$

where:

- b_{Ai} = adjusted width of the i^{th} lamination,
- E_i = modulus of elasticity of the i^{th} lamination,
- E_* = transformed modulus of elasticity and
- b_i = width of the i^{th} lamination.

The elastic flexural formulas then can be used with slight modification. The bending stress in the cross section is represented by:

$$\sigma_{bi} = \frac{E_i}{E_*} \frac{My}{I_t} \quad (3.3)$$

where:

- σ_{bi} = normal bending stress in the i^{th} lamination,
- M = bending moment applied at the cross section,
- y = distance from the neutral axis to the point in question and
- I_t = moment of inertia of the transformed cross section.

An element of the original simple composite beam, Figure 3.1(a), is removed and examined in greater detail in Figure 3.2(a). This cut has length dx and cross sectional properties identical to the original beam shown in Figure 3.1(b). The element is subjected to a moment M on the left side and an opposing moment on the right side $M + dM$. The bending stress is superimposed on Figure 3.2(a). Note the discontinuity in the stress distribution corresponding to the different values of E , with the slope becoming steeper as E increases. Both of these properties are characterized by Equation 3.3. The shaded area in Figure 3.2(a) is now examined in greater detail in Figure 3.2(b).

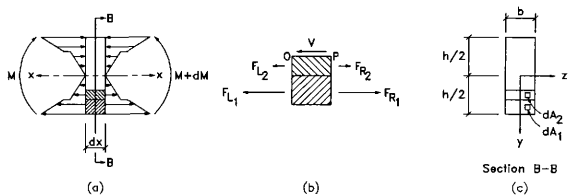


Figure 3.2: Stresses, forces and moments on the composite cross section.

The bending stresses are resolved into component forces F in Figure 3.2(b). The shear V acting parallel to the line OP can be found using simple statics as follows:

$$\sum F_x = 0 = F_{R_1} + F_{R_2} - F_{L_1} - F_{L_2} - V_{OP} \quad (3.4)$$

where:

$$\begin{aligned} F_{R_i} &= \text{resultant bending force on the right side in the } i^{\text{th}} \text{ lamination,} \\ F_{L_i} &= \text{resultant bending force on the left side in the } i^{\text{th}} \text{ lamination and} \\ V_{OP} &= \text{shear force acting parallel to line } OP. \end{aligned}$$

Rearranging terms to solve for V_{OP} :

$$V_{OP} = F_{R_1} + F_{R_2} - F_{L_1} - F_{L_2} \quad (3.5)$$

The bending stress (Equation 3.3) can be integrated over each area A_i ; thus, yielding the resultant component forces over their respective areas. These resultant forces can then be substituted into Equation 3.5 to form Equation 3.6. Figure 3.2(c) is a section removed from 3.2(a) illustrating the infinitesimal area dA_i . The area of integration A_i must be changed as the modulus of elasticity changes.

$$\begin{aligned}
 V_{OP} = & \int_{A_1} \frac{E_1}{E_*} \frac{(M+dM)y}{I_1} dA_1 + \int_{A_2} \frac{E_2}{E_*} \frac{(M+dM)y}{I_1} dA_2 \\
 & - \int_{A_1} \frac{E_1}{E_*} \frac{My}{I_1} dA_1 - \int_{A_2} \frac{E_2}{E_*} \frac{My}{I_1} dA_2
 \end{aligned} \tag{3.6}$$

where: A_i = area of integration of the i^{th} lamination and

Equation 3.6 can be simplified as shown in Equation 3.7.

$$V_{OP} = \int_{A_1} \frac{E_1}{E_*} \frac{dMy}{I_1} dA_1 + \int_{A_2} \frac{E_2}{E_*} \frac{dMy}{I_1} dA_2 \tag{3.7}$$

The shear stress τ_{OP} can be found by dividing the shear force acting parallel to line OP by the area that it acts over as follows:

$$\tau_{OP} = \frac{V_{OP}}{dx b} \tag{3.8}$$

where:

dx = length of cut in the simple composite beam and
 τ_{OP} = shear stress acting parallel to the line OP .

Equation 3.9 is the result when Equation 3.7 is substituted into Equation 3.8.

$$\tau_{OP} = \frac{E_1}{E_*} \frac{dM}{dx} \frac{1}{I_1 b} \int_{A_1} y dA_1 + \frac{E_2}{E_*} \frac{dM}{dx} \frac{1}{I_1 b} \int_{A_2} y dA_2 \tag{3.9}$$

Equation 3.9 can be simplified by noting the shear force V is the derivative of the moment dM/dx , and the area integral is commonly known as the first moment of the area Q .

Equation 3.10 gives the shear stress in the simple composite beam acting parallel to line OP .

$$\tau_{OP} = \frac{E_1}{E_*} \frac{VQ_1}{I_*b} + \frac{E_2}{E_*} \frac{VQ_2}{I_*b} \quad (3.10)$$

where: Q_i = first moment of the area of the i^{th} lamination.

Equation 3.10 can be expanded to the general case for any number of laminations, shown by Equation 3.11. This is the general form of the equation for shear stress at any point λ , along the depth of the beam.

$$\tau_\lambda = \frac{V \sum_{k=1}^{\lambda} E_k Q_k}{E_* I_* b} \quad (3.11)$$

where: τ_λ = shear stress at any point λ along the length and depth of the beam.

A similar form of this equation can be found in Allen and Haisler (1985) in the advanced beam section.

SHEAR DEFLECTION DERIVATION FOR COMPOSITE BEAMS

Once a general equation for shear stress is derived, the internal energy can be found by substituting Equation 3.11 into the second part of Equation 2.1, yielding Equation 3.12.

$$U_s = \frac{1}{2G} \iiint \left(\frac{V}{E_* I_* b} \right)^2 \left(\sum_{k=1}^{\lambda} E_k Q_k \right)^2 dz dy dx \quad (3.12)$$

Applying Castigliano's Theorem (Equation 2.2) to Equation 3.12 results in Equation 3.13.

$$\delta_{x,v} = \frac{1}{G} \int_0^L \int_{-\frac{h}{2}}^{\frac{h}{2}} \int_0^b \frac{V}{(E_* I_i b)^2} \left(\sum_{k=1}^j E_k Q_k \right)^2 \frac{\partial V}{\partial F_x} dz dy dx \quad (3.13)$$

Integrating across the base yields:

$$\delta_{x,v} = \frac{1}{G} \int_0^L \int_{-\frac{h}{2}}^{\frac{h}{2}} \frac{V}{(E_* I_i)^2 b} \left(\sum_{k=1}^j E_k Q_k \right)^2 \frac{\partial V}{\partial F_x} dy dx \quad (3.14)$$

Equation 3.14 can be integrated numerically by expressing it in the form of Equation 3.15. The integrals are replaced with summations and the partial derivatives are replaced by v_i , which is the shear component of a unit load applied at midspan. The shear modulus, G_i , is placed inside the summations so it can vary along the length and depth of the beam. The E_* is removed from inside the summations because it is constant across the beam length and depth.

$$\delta_{x,v} = \frac{1}{E_*} \left[\sum_{i=1}^{ncutx} \frac{V_i v_i}{I_i^2} \left[\sum_{j=1}^{ncuty} \frac{\left(\sum_{k=1}^j E_{ik} Q_k \right)^2}{b_j G_{ij}} \Delta y \right] \Delta x \right] \quad (3.15)$$

where:

- $\delta_{x,v}$ = shear deflection at point x ,
- E_* = transformed modulus of elasticity,
- $ncutx$ = number of intervals along the x -axis,
- V_i = shear force at i ,
- v_i = shear force at i due to unit load at x ,
- I_i = moment of inertia of the transformed cross section at i ,
- $ncuty$ = number of intervals along the y -axis and
- E_{ik} = modulus of elasticity of the k^{th} lamination at i ,
- Q_k = first moment of the area of the k^{th} lamination,
- b_j = actual width of the j^{th} lamination,

- G_{ij} = shear modulus of the j^{th} lamination at i ,
 Δx = width of intervals along the x -axis,
 Δy = width of intervals along the y -axis.

SUMMARY

An equation was derived to calculate the shear stress at any point along the length and depth of a composite beam. This equation then was extended using energy methods, resulting in an equation that characterized the deflection from any arbitrary flexural loading condition. Assumptions and limitations to the developed equations are discussed next.

Assumptions

The assumptions that led to the derivation of Equations 3.11 and 3.15 are as follows:

1. The shear force on the beam acts parallel to the shear stresses.
2. The shear stresses act uniformly across the width of the beam.
3. The material is linear elastic homogeneous and is only subjected to small displacements.
4. Deformations are about the plane of bending (i.e. no lateral-torsional buckling).

Limitations

A limitation of the model is that the shear stress formula (Equation 3.11) is limited to beams that are deeper than they are wide. When $b=h$, the true maximum shear stresses can be significantly larger (13% for a homogeneous beam) than what Equation 3.11 predicts (Gere and Timoshenko, 1984). This underprediction of shear stress would also

cause an error in the amount of shear deflection predicted by Equation 3.15 for a composite beam.

CHAPTER IV

MODEL VERIFICATION

Verification of a model is simply to determine if the model performs as intended. There are numerous techniques that can be used to verify the shear deflection model for composite beams developed in Chapter III (Equation 3.15). One possible comparison would be to use a finite element (FE) method to characterize the deflection caused by a certain loading condition. The problem with this technique is the input parameters, i.e. material properties, are neither completely characterized for every wood species grouping nor understood in the general area surrounding naturally occurring strength reducing flaws (e.g. knots and grain deviations). If a discrepancy is found between the FE model and Equation 3.15 it is not known if the error is with the material property assumption or with the shear deflection model. The verification approach used here is to compare Equation 3.15 with other energy methods. By comparing the shear deflection model with different energy method models, a measure of confidence can be obtained if the models compare favorably.

MODEL COMPARISON

Symmetric Two-Point Loaded Homogeneous Rectangular Beam

The first comparison conducted is for a homogeneous rectangular beam that is simply supported, and is loaded by two symmetrically placed loads. This case scenario is fairly simple; therefore, the exact theoretical solution was obtained by using energy methods. The predicted deflection from Equation 3.15 was then compared to the exact solution. The two-point loading was selected because it is a more general loading case than a single concentrated load located at midspan. Figure 4.1 is a graphical representation of this case scenario with the shear (V) and moment (M) diagrams plotted beneath the beam schematic diagram. The beam is loaded with symmetric two-point loads $P/2$, located at a distance

a from the ends of the beam. A fictitious concentrated load Q is applied at midspan so deflection could be found at that point. The width and depth of the beam are b and h , respectively. Two local coordinate systems are defined (x_1 and x_2) to simplify characterizing the V and M equations that are used in the deflection calculations.

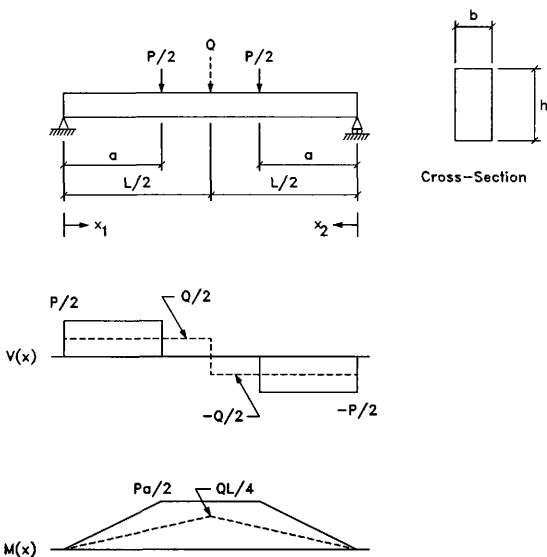


Figure 4.1: Shear and moment diagrams for a homogeneous beam.

The moment and shear equations and the corresponding partial derivatives must be broken into four separate equations because of discontinuities, and is written as follows:

$x_1 : 0 \text{ to } a$

$$M(x_1) = \frac{Px_1}{2} + \frac{Qx_1}{2}$$

$$\frac{\partial M}{\partial Q} = \frac{x_1}{2}$$

$$V(x_1) = \frac{P}{2} + \frac{Q}{2}$$

$$\frac{\partial V}{\partial Q} = \frac{1}{2}$$

 $x_1 : a \text{ to } L/2$

$$M(x_1) = \frac{Pa}{2} + \frac{Qx_1}{2}$$

$$\frac{\partial M}{\partial Q} = \frac{x_1}{2}$$

$$V(x_1) = \frac{Q}{2}$$

$$\frac{\partial V}{\partial Q} = \frac{1}{2}$$

 $x_2 : 0 \text{ to } a$

$$M(x_2) = \frac{Px_2}{2} + \frac{Qx_2}{2}$$

$$\frac{\partial M}{\partial Q} = \frac{x_2}{2}$$

$$V(x_2) = -\frac{P}{2} - \frac{Q}{2}$$

$$\frac{\partial V}{\partial Q} = -\frac{1}{2}$$

 $x_2 : a \text{ to } L/2$

$$M(x_2) = \frac{Pa}{2} + \frac{Qx_2}{2}$$

$$\frac{\partial M}{\partial Q} = \frac{x_2}{2}$$

$$V(x_2) = -\frac{Q}{2}$$

$$\frac{\partial V}{\partial Q} = -\frac{1}{2}$$

Equation 4.1 is the energy method procedure with the shear and moment equations substituted into Equation 2.3 to find the midspan deflection. The virtual load Q applied at the midspan is a fictitious load and is equal to zero; therefore, it was excluded from

the deflection calculations; although, the partial derivatives associated with Q must be included.

$$\begin{aligned} \delta &= \frac{1}{EI} \int_0^a \frac{Px_1}{2} \frac{x_1}{2} dx_1 + \frac{k}{GA} \int_0^a \frac{P}{2} \frac{1}{2} dx_1 + \\ &\quad \frac{1}{EI} \int_a^{\frac{L}{2}} \frac{Pa}{2} \frac{x_1}{2} dx_1 + \frac{k}{GA} \int_a^{\frac{L}{2}} 0 dx_1 + \\ &\quad \frac{1}{EI} \int_0^a \frac{Px_2}{2} \frac{x_2}{2} dx_2 + \frac{k}{GA} \int_0^a \left(-\frac{P}{2}\right) \left(-\frac{1}{2}\right) dx_2 + \\ &\quad \frac{1}{EI} \int_a^{\frac{L}{2}} \frac{Pa}{2} \frac{x_2}{2} dx_2 + \frac{k}{GA} \int_a^{\frac{L}{2}} 0 dx_2 \end{aligned} \tag{4.1}$$

where:

- P = sum of the two symmetrically placed loads,
- a = distance from the two-point load to the end of the beam and
- L = distance between the beam reactions.

After integration and algebraic simplification, the final deflection equation for a simply supported two-point loaded homogeneous beam is expressed as follows:

$$\delta = \frac{Pa}{48EI} (3L^2 - 4a^2) + \frac{kPa}{2GA} \tag{4.2}$$

As before, the first term represents the bending component of deflection and the second term represents the shear component.

The following beam dimensions are assumed for this verification: $L = 456$ in., $a = 180$ in., $b = 5.125$ in., and $h = 24$ in. Other assumptions include: the beam is homogeneous

with $E = 2.0 \times 10^6$ psi, $G = (E/16)$ and $P = 1000$ lbs. The form factor (k) was equal to 1.20 since the cross section was rectangular. The bending term from Equation 2.4 and the composite shear deflection equation (Equation 3.15) were encoded in a FORTRAN routine (see Appendix A). Additional parameters needed for the algorithm were $ncutx = 76$ with a $\Delta x = 6$ in. and $ncuty = 16$ with a $\Delta y = 1.5$ in.

Table 4.1 displays the results of the two methods. The two models compared favorably for both bending and shear. Both bending deflection and shear deflection predicted from the model were consistent to four significant digits. The small error could be minimized even more if $ncutx$ is increased; however, the error is less than three hundredths of a percent. This error is insignificant since the variability of all material properties prevent the actual deflection from being calculated to this much accuracy. The numbers were carried out to six significant digits for comparison reasons, not to imply false accuracy.

Table 4.1: Results from the symmetric two-point loaded homogenous rectangular beam test scenario.

Method	bending deflection (in)	shear deflection (in)	total deflection (in)
Exact Solution*	0.156 951	0.007 024	0.163 975
Finite difference†	0.156 997	0.007 024	0.164 021
error (%)	0.029	0.0	0.028

* Calculated using Equation 4.2

† FORTRAN algorithm using Equations 2.4 and 3.15 (see Appendix A)

Uniformly Loaded Homogeneous Rectangular Beam

Beams are often subjected to uniform and concentrated loads in design applications. Hence, it is important to predict total deflection for both types of loading conditions. The shear distribution and moment distributions for a uniformly loaded beam are one-degree higher polynomials than for concentrated loads. Since shear and bending deflections are

related to their respective distributions, the numerical integration of Equation 3.15 could be erroneous for higher-order loading such as uniform loading; therefore, a homogeneous uniformly loaded beam is analyzed as the second beam test case.

The exact theoretical equations for bending and shear deflection were derived for a homogeneous, uniformly loaded beam using energy methods similar to the procedure for developing Equation 4.2. Equation 4.3 represents the final results of this procedure.

$$\delta = \frac{5}{384} \frac{wL^4}{EI} + \frac{kWL^2}{8GA} \quad (4.3)$$

where w = a uniform load.

The uniform load, w , for this test case was taken as 10 lbs/in. All other parameters for the FORTRAN algorithm were identical to the two-point loading scenario discussed previously. Table 4.2 presents the results from this case scenario. The bending deflection predictions were consistent to three significant digits and the shear deflection predictions were consistent to four significant digits.

Table 4.2: Results from the uniformly loaded homogeneous rectangular beam test scenario.

Method	bending deflection (in)	shear deflection (in)	total deflection (in)
Exact Solution*	0.476 784	0.020 286	0.497 070
Finite difference†	0.476 850	0.020 286	0.497 136
error (%)	0.014	0.0	0.013

* Calculated using Equation 4.3

† FORTRAN algorithm using Equations 2.4 and 3.15 (see Appendix A)

Although the deflection calculation lost one significant digit from the two-point loading case, the error between the model and the exact predicted results decreased. From a practical standpoint this error is insignificant; however, better accuracy could be achieved by increasing $ncutx$ and decreasing Δx . The shear deflection model performed well for both rectangular homogeneous case studies. The two different loading conditions did not have a significant effect on the accuracies of the shear deflection model.

Homogeneous I-Beam

In the next case study, the cross section of the beam is altered. A cross section that is popular for structural members is the I-beam. This is an efficient section in terms of bending and deflection because the majority of the material is located at a farther distance from the neutral axis than a solid section with the same amount of material. Figure 4.2 illustrates the cross sectional dimensions of a commercially produced wood I-beam.

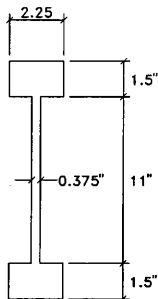


Figure 4.2: Cross sectional dimensions of a commercially produced wood I-beam.

The length of the beam was assumed to be 252 in. and was loaded at third points ($a = 84$ in.) with $P = 500$ lbs. The material properties for this homogeneous beam were

assumed as $E = 2.0 \times 10^6$ psi and $G = (E/16)$. The FORTRAN algorithm had additional parameters of $ncutx = 42$ with a $\Delta x = 6$ in. and $ncuty = 28$ with a $\Delta y = 0.5$ in. To assure accuracy of the model, cuts along the y-axis must be made at discontinuities in the cross sections, such as changes in E and changes in the width of the member; therefore, more intervals were required along the y-axis for the I-beam than the rectangular beam because of the cross sectional geometry. The shear deflection model was compared with Equation 4.2 with a modified k factor. Using the Orosz (1970) method to calculate k for an I-beam (see Appendix B), it was found that $k = 2.134\ 718$. Table 4.3 presents the results from this case study. The shear and bending deflection models both compare well to the model using Equation 4.2 and the Orosz k factor.

Table 4.3: Results from homogeneous I-beam test scenario.

Method	bending deflection	shear deflection	total deflection
	(in)	(in)	(in)
Theoretical Soln.*	0.231 627	0.032 978	0.264 605
Finite difference†	0.231 633	0.032 978	0.264 611
error (%)	0.003	0.0	0.002

* Calculated using Equation 4.2 and $k = 2.134\ 718$ (Orosz, 1970) (see Appendix B)

† FORTRAN algorithm using Equations 2.4 and 3.15 (see Appendix A)

Composite I-Beam

A variation on the homogeneous I-beam that improves its efficiency even more is producing it from two different materials. Since I-beams are often used in designs where deflection or bending stress are the limiting factors, such as floors and ceilings, manufacturers make the flanges out of high quality, stiff material; thus, increasing the strength and stiffness of the beam. I-beams can be made with lower quality material in the web since longer spans usually are not governed by shear failures. Predicting bending deflection for a composite beam simply requires using the homogeneous equation with

slight modification. The cross section is transformed to a homogeneous material and the moment of inertia is calculated for the transformed cross section. The E value used in the deflection equation is the E for the transformed homogeneous material. The shear deflection is also similar to the homogeneous case. Orosz's (1970) method was used to calculate k for a composite I-beam (see Appendix B). The cross section for this method is transformed to the E of the web with the area of the transformed cross section being substituted for A . The value for G is assumed to be $E_{web}/16$. This case study assumes the same parameters as the homogeneous I-beam with the only differences being that the E of the flange is assumed to be 3.0×10^6 psi and the E of the web is assumed to be 1.0×10^6 psi. The form factor was calculated as 4.621 403. Table 4.4 displays a comparison between the shear deflection model and Equation 4.2 with the modified k factor.

Table 4.4: Results from composite I-beam test scenario.

Method	bending deflection (in)	shear deflection (in)	total deflection (in)
Theoretical Soln.*	0.169 776	0.063 704	0.233 480
Finite difference†	0.169 781	0.063 704	0.233 485
error (%)	0.003	0.0	0.002

* Calculated using Equation 4.2 and $k = 4.621\ 403$ (Orosz, 1970) (see Appendix B)

† FORTRAN algorithm using Equations 2.4 and 3.15 (see Appendix A)

Once again, the shear deflection model performed well, compared to the theoretical deflection, for a composite I-beam. An interesting observation between the difference in the homogeneous I-beam and the composite I-beam should be pointed out. Producing an I-beam that has a flange 50% stiffer than the homogeneous case only reduced bending deflection by 36%; however, decreasing the E of the webs by 50% nearly doubled the shear deflection. This confirms intuition, because the maximum shear stress in the beam is located at the neutral axis which is made from the less stiff material.

Composite Glulam Beam

The final case study is for a composite glued-laminated timber (glulam) beam. Many of the beams specified by AITC 117-Manufacturing (1988) are not symmetrically balanced about the neutral axis. Figure 4.3 represents a layup for a 24F-V4 beam that Hernandez (1991) used in his research. This is one of many beam combinations specified by AITC.

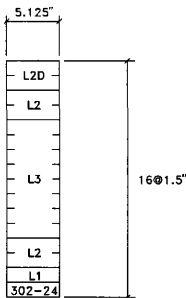


Figure 4.3: 16 lamination 24F-V4 glulam beam layup.

Glulam beam manufacturers, like I-beam manufacturers, want to optimize the material placed in a glulam beam to best utilize their lumber resource and still maintain strength and stiffness design values. They achieve the same goal by placing the higher quality wood farthest from the neutral axis and the lower quality material in the core. The 24F-V4 beam contains 50% of the abundant lumber graded L3 and only one lamination of the scarce, high quality lumber graded as 302-24. This high quality zone in the bottom of Figure 4.3 is referred to as the tension lamination and is located on the tension face of the beam. This lumber grade limits the strength reducing characteristics to small knots and small grain deviations. This unbalanced layup changes the position of the neutral axis, so it is not necessarily in the middle of the cross section. Table 4.5 list the E

values assumed for the five lumber grades for the test case scenario. These values were taken from Hernandez's (1991) data. These values correspond to the median E values for their respective grades.

Table 4.5: Modulus of elasticity values assumed for the 24F-V4 glulam beam.

Lumber Grade	Modulus of Elasticity* (Mpsi)
302-24	2.996
L1	2.710
L2D	2.557
L2	2.205
L3	1.985

* Median E values (Hernandez, 1991)

The deflection of the glulam beam was calculated similarly to the I-beam. The theoretical deflection was calculated using Equation 4.2 with several modified parameters. The dimensions of the beam were identical to the rectangular homogeneous loading case with $P = 1000$ lbs. The cross section was transformed to the average of the E values for the 16 different laminations. The moment of inertia was calculated for the transformed cross section. The k factor was calculated using a method that was developed by Mansour and Gopu (1990) to be 1.272 750 (see Appendix C). The shear modulus was assumed to be equal to $E_{\text{mean}}/16$ and the A term was equal to the gross cross sectional area, which is also equal to the transformed cross sectional area. This modified equation was compared to the shear deflection model and the results are displayed in Table 4.6.

Table 4.6: Results from composite glulam beam test scenario.

Method	bending deflection (in)	shear deflection (in)	total deflection (in)
Theoretical Soln.*	0.127 039	0.006 712	0.133 751
Finite difference†	0.127 076	0.006 722	0.133 798
error (%)	0.029	0.149	0.035

* Calculated using Equation 4.2 and $k = 1.272\ 750$ (Mansour and Gopu, 1990) (see Appendix C)

† FORTRAN algorithm using Equations 2.4 and 3.15 (see Appendix A)

The bending deflection error was consistent with the other test case scenarios. The shear deflection error was larger; however, the error for the shear deflection model is less than two-tenths of a percent which is practically insignificant. In this case, the error term was reduced by increasing the number of intervals along the y-axis. By increasing *ncury* to 48, the error in the prediction was reduced to 0.045%. This error in the prediction was caused by the unsymmetric cross section. The centroid does not correspond to one of the increments; therefore, the discontinuity at the centroid was skipped. It would be most favorable for an increment to correspond to the centroid; however, this is infeasible for all beam layouts. Although the accuracy increased as the number of increments increased, the error in the original prediction was small and had little effect on the total deflection prediction.

SUMMARY

The shear deflection model developed in Chapter III (Equation 3.15) was verified for a variety of beam scenarios and compared to classical methods. The error in the prediction associated with the shear deflection model was negligible for rectangular homogeneous beams loaded by either two-point symmetric loading or uniform loading, as well as for homogeneous and composite I-beams loaded with symmetric two-point loading. The error between the theoretical shear deflection and the shear deflection model for a composite

glulam beam loaded with a two-point symmetric load was found to be less than two-tenths of a percent. The error term can be further reduced if the number of intervals along the y-axis is increased for the numerical integration.

The shear deflection model was verified through comparison with existing published shear deflection models. This model is more flexible because it can be used for either rectangular or non-rectangular shaped beams; whereas, other beam models are limited to either composite glulam beams or I-beams.

CHAPTER V

MODEL VALIDATION

Validation of a model is to determine whether the model accurately represents the "real-world" system which it is intended to characterize. The composite shear deflection model (Equation 3.15) was validated with a set of data collected by Hernandez (1991). Lumber data were used as input to the deflection model which back-solved for glulam beam apparent E . The results were compared to actual glulam beam E 's measured in the laboratory.

EXPERIMENTAL PROCEDURE

Hernandez's (1991) and Hernandez et al.'s (in press) work on a probabilistic glulam beam model (called PROLAM) was done concurrently with an extensive research program undertaken by the American Institute of Timber Construction (AITC) that tested full size glulam beams. This research program was conducted for a variety of reasons, including validation of glulam beam models. Before the beams were fabricated, the laminating stock was run through a continuous stress grading machine to obtain E profiles for each piece of lumber. These pieces then were stamped with an identification number so they could be identified in the glulam beam after fabrication. A group of thirty 16-lamination 24F-V4 Douglas-fir glulam beams were tested for this research program. The 24 in.-deep beams were manufactured to a length of 40 ft. using nominal 2 x 6 in. Douglas-fir laminating lumber. After fabrication, the beams were planed to a final width of 5.125 in. These beams were destructively tested at the U.S. Forest Products Laboratory under symmetric two-point loading. The beams spanned 38 ft. between the reactions with a distance of 8 ft. between the load-heads. The beams were restrained from buckling out of plane. During testing, the apparent E was measured for each beam.

The E profiles recorded from the continuous lumber tester (CLT) data were averaged for each two-foot lumber segment. Beam maps were constructed using the two-foot average E_{CLT} . Cross sectional profiles were then taken at a one foot interval and matrices of numbers were recorded in data files. The dimension of the matrices were 39 by 16, representing 39 one foot intervals and 16 laminations. One beam map could not be constructed due to a data collection problem; therefore, the sample size was 29.

ADJUSTMENT OF LUMBER E VALUES - METHOD 1

Model development

A FORTRAN program (Appendix D) was written to analyze the array of CLT data. The program first transformed the array of E_{CLT} to two foot static bending modulus of elasticity, E_s , using the following equation (Hernandez, 1991).

$$E_s = 1.3224 * E_{CLT} - 0.2344 \quad (5.1)$$

where:

- E_s = two-ft static bending E and
- E_{CLT} = raw CLT- E values averaged over a two-ft segment.

It should be noted that Equation 5.1 is an empirical regression model developed from an independent lumber sample. The E_{CLT} used to develop Equation 5.1 was collected at a different time and a different CLT machine than the lumber profiles collected for this research; however, the CLT machines were calibrated approximately the same. This test scenario was conducted to analyze the robustness of Equation 5.1. This program simulates loading the beams with a symmetrically placed two-point load with an arbitrary load at the same location where the actual beams were loaded. The deflections of the beams were estimated using the first term of Equation 2.4 and Equation 3.15. After the deflection was found, the beam apparent E was backed-solved for using the classic deflection (bending deflection only) equation for symmetric two-point loading.

Test Results

The first case scenario assumed an E/G ratio of 16, which is the traditional value for Douglas-fir lumber found in the Wood Handbook (USDA, 1987). Figure 5.1 illustrates a graph of the measured E versus predicted E .

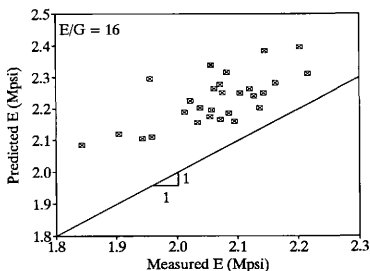


Figure 5.1: Predicted E versus measured E for 24F-V4 Douglas-fir beams ($E/G = 16$).

The predicted E was higher than the measured E for all 29 beams. The error ranged from 3.18 to 17.38% with an average of 8.28%. Appendix E contains the data for the actual and predicted E values for the test beams. A paired t-test (Walpole and Myers, 1978) was performed on the null hypothesis that the two means were equal. The t-test statistic was calculated as 13.46 which is greater than the critical t value of 1.70 at a significance level of 5 percent and 28 degrees of freedom; thus, rejecting the null hypothesis.

In The next case scenario, E/G ratio was altered. Chui (1991) suggested that an E/G ratio for low quality wood ranged from 25 to 30 and an E/G ratio of 20 was more reasonable

for straight-grained wood. Since the lumber graded L3 consisted of relatively low quality lumber, an E/G ratio of 30 was assumed and the other lumber grades were assumed to have an E/G ratio of 20. Figure 5.2 illustrates the data from this test.

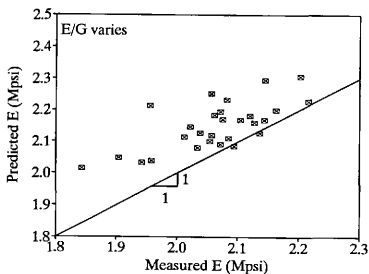


Figure 5.2: Predicted E versus measured E for 24F-V4 Douglas-fir beams ($E/G = 20$ for all laminations except L3 where $E/G = 30$).

The error for this test ranged from -0.43 to 13.14% with an average of 4.42% . The t -statistic was calculated as 7.32 for the two means. Once again a statistically difference was found between the means.

ADJUSTMENT OF LUMBER E VALUES - METHOD 2

A possible source of error is the transformation between E_{CLT} to E_s . This regression equation was developed for a different sample of lumber (Richburg, 1989) than the sample used to fabricate the glulam beams. A CLT is a machine that subjects lumber to a concentrated load at midspan with a span of 48 in. The lumber is forced to undergo a fixed deflection and the load required to cause this deflection is continuously measured

as the specimen is fed through the machine. Then the E is inferred from the continually measured load. The regression equation (Equation 5.1) that transforms the E_{CLT} to E_s takes two factors into account: span and shear. The equation transforms from a span of 48 in. to a span of 24 in., and the E_{CLT} data include shear deflection; whereas, the E_s is calculated from pure bending deflection. Since Equation 5.1 is an empirical relationship and it was developed from a different lumber data set, it is not necessarily valid for the lumber sample used to fabricate the glulam beams.

A transformation that should be analyzed uses a regression equation developed at approximately the same time that the E -profiles were collected for the laminating lumber. This regression equation was developed by Galligan (Bender, 1990) for the CLT machine in which the E -profiles were obtained. It relates E_{CLT} to long-span static bending modulus of elasticity (E_{LS}) as follows:

$$E_{LS} = 1.227 * E_{CLT} - 0.191 \quad (5.2)$$

where: E_{LS} = long-span static bending E .

This equation cannot directly parallel Equation 5.1, because it transforms to E_{LS} , not E_s . An equation was developed (see Appendix F) that transforms the E data from long-span to short-span. This equation can be written as follows:

$$E_s = 1.142 * E_{LS} - 0.219 \quad (5.3)$$

Equations 5.2 and 5.3 were substituted into the FORTRAN code in place of Equation 5.1, and the same analysis was repeated. The paired t-test statistic for $E/G = 16$ was calculated as 9.37. This again indicates significant difference between the two means at a 5% level of confidence. This scenario overpredicted E in all cases with the range of error from 0.62 to 15.03%, with an average of 8.93%. In the next study, the E/G ratio was assumed to be equal to 20 for all lumber grades except L3 where it was assumed to

be 30. The paired t-test statistic equaled 3.37 indicating statistical significance between the two mean values, and the errors ranged from -2.96 to 10.79% with an average of 2.11% .

ADJUSTMENT OF LUMBER E VALUES - METHOD 3

Equation 5.3 was developed on a two-ft shear-free bending test in which data indicate (see Appendix F) that the average two-ft E_3 for lumber is larger than E_{LS} ; however, Kline, et al. (1986) suggest that the average of the short span segments should be close to the E_{LS} . This could possibly indicate that the procedure for measuring E_3 used in Equations 5.1 and 5.3 gives higher results than expected due to an unexplained experimental phenomenon. Therefore, the next case scenario only uses Equation 5.2 which transforms E_{CLT} to E_{LS} . The results for this test case were the most favorable. At an E/G ratio of 16, the paired t-test statistic was calculated as 2.76 which is the closest to the critical value of 1.70 at a 5% level of confidence for all case scenarios. The percent error ranged from -3.09 to 10.22% with an average of 1.71% . The mean of the predicted E was only 33 800 psi higher than the mean of the actual measured E . The next test varied the E/G ratio as before. This yielded a t-statistic of -3.40 and the errors ranged from -6.447 to 6.237% with an average of -1.91% . Although there was statistical significant difference between the actual and the predicted E values, there was no practical difference for an E/G ratio of 16 with Equation 5.2 used as the E transformation equation.

Figure 5.3 illustrates three different empirical cumulative distribution functions (CDF). The middle CDF represents the actual data. The CDF on the right represents the predicted E for the test case scenario of $E/G = 16$ and using Equation 5.2 as the transformation equation. The CDF on the left side of the predicted CDF is for an E/G ratio that equals 20 for all lumber samples except L3 in which $E/G = 30$.

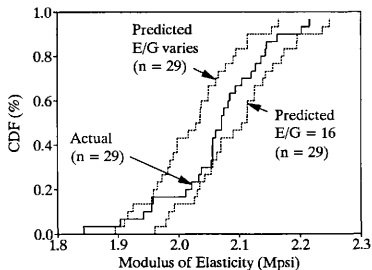


Figure 5.3: Empirical cumulative distribution function for various case scenarios.

SUMMARY

Close agreement was found between actual and predicted beam apparent E . Less than two percent difference was observed between the two mean values. Although a paired t-test indicated significant differences between the means, the variability of the predicted and the actual E 's were small; thus, making it easy to reject the null hypothesis that the two means were identical. The regression equation that relates E_{CLT} to E_s appears to be in error. The regression equation relating E_{CLT} and E_{LS} gave the best results for all cases studied. This could be because the regression equation was developed at approximately the same time the lumber profiles were collected from the CLT machine. Equations 5.1 and 5.3 were developed with independent lumber samples, and they consistently overpredict E_s . It appears the calibration equation for the CLT machine varies over time and from machine to machine; therefore, it is recommended to periodically collect test data that relate E_{CLT} and E_{LS} . A possible source of error could be the way that shear stress is modeled. It has been shown by numerous researchers (Doyle and Markwardt,

1966;1967, Palka and Barrett, 1985 and Chui, 1991) that G is a random variable; however, for this model it was assumed to be a constant ratio to E throughout the lamination for lack of a better procedure to model G .

CHAPTER VI

MODEL IMPLEMENTATION

The shear deflection model developed in Chapter III (Equation 3.15) was verified for a variety of test case scenarios in Chapter IV. The deflections predicted with the model compared well both to theory and to published shear deflection models (Orosz, 1970 and Mansour and Gopu, 1990). The model compared closely to actual test data in Chapter V, with an error of less than two percent between the averages of actual and predicted E was observed. Since the model compared favorably to existing deflection methods and to actual test data, it was implemented into a probabilistic glulam beam model developed by Hernandez et al. (in press), called PROLAM.

EXISTING GLULAM MODEL: PROLAM

PROLAM is a stochastic model that simulates glulam beam performance. This model simulates glulam beam fabrication and generates random values of E and tensile strength (T) for each two-foot lumber segment in the beam. These E and T values are spatially correlated along the lengths of the individual pieces of lumber. The simulated pieces of lumber are joined together with finger joints that also are assigned E and T values. This model predicts the strength of the beam in bending, referred to as modulus of rupture (MOR), using a transformed section analysis. The E for the beam is calculated using a finite difference approximate method developed by Hilson et al. (1990, 1988) and Pellicane and Hilson (1985), represented by Equation 2.4.

PROLAM was validated with the 30 beams discussed in Chapter V for MOR; however, the simulated E values were approximately 14% high (Hernandez et al., in press). Since Equation 2.4 only approximates the shear deflection for composite beams a more accurate model was implemented into PROLAM (Equation 3.15).

PROLAM Refinements

PROLAM has a subroutine that calculates the transformed section at specific increments, Δx , then it repeats the transformed section at each finger joint location in the tension zone of the beam. The original deflection model developed by Hilson et al. (1990, 1988) and Pellicane and Hilson (1985) was placed in this subroutine. The composite shear deflection model is more complex; therefore, when it was substituted into PROLAM, it was placed in a separate subroutine. Another addition to PROLAM was allowing the E/G ratio to vary for the different lumber grades. Although this is not completely stochastic, the E/G ratio can vary across the cross section instead of being held to a constant ratio of E/G .

SENSITIVITY ANALYSES

Several sensitivity analyses were analyzed using PROLAM with the composite shear deflection model implemented. The beams simulated were identical to the validation beams discussed in Chapter V. The sensitivity in the numerical integration was studied as well as the effect of different shear deflection models. The sensitivity of E/G also was studied.

Effect of Length Increment Size

The number of increments along the length of the beam were chosen to be 500, 250, 100, 50, 38, 25 and 10 resulting in increment sizes of 0.912, 1.824, 4.560, 9.120, 12.00, 18.24 and 45.60 in., respectively. A total of 1000 beams were simulated with the same random number seed for the seven computer runs as a variance reduction technique (Law and Kelton, 1991). Average beam E 's for the various beam simulations are summarized in Table 6.1.

Table 6.1: Effect of length increment on apparent modulus of elasticity.

<i>ncutx</i>	Δx (in)	apparent E^* (Mpsi)	error [†] (%)
500	0.912	2.330	—
250	1.824	2.331	0.043
100	4.560	2.332	0.086
50	9.120	2.335	0.215
38	12.00	2.333	0.129
25	18.24	2.343	0.558
10	45.60	2.334	0.172

* Predicted using PROLAM

† Assumes *ncutx* = 500 is basis for comparison

For numerical integration, the accuracy increases as the number of increments becomes larger, to a certain point where round off error begins to dominate (Chapra and Canale, 1988); therefore, it was judged to use *ncutx* = 500 as the basis for the comparisons. The errors for all cases studied were less than one percent. Although the error was small for 10 increments, this would be a poor number to choose because Δx is larger than the two-foot lumber property cells; therefore, a very low E segment could be skipped. Furthermore, this analysis does not take into account the effect that *ncutx* has on MOR , only E . The error is small for all the test cases; therefore, E is fairly insensitive to the number of increments along the length of the beam. An increment of $\Delta x = 12$ in. was selected to further analyze the validation beams.

Effect of Depth Increment Size

A similar sensitivity analysis was performed for the number of increments in the y -direction. The number of intervals, *ncuty*, was set at 160, 48 and 16 resulting in

increment sizes of 0.150, 0.500 and 1.500, respectively. The results from this sensitivity analysis are given in Table 6.2.

Table 6.2: Effect of depth increment size on apparent modulus of elasticity.

<i>ncuty</i>	Δy (in)	apparent E^* (Mpsi)	error [†] (%)
160	0.150	2.333	—
48	0.500	2.333	0.0
16	1.500	2.333	0.0

* Predicted using PROLAM

† Assumes *ncuty* = 160 is basis for comparison

There was no effect on the average apparent E for the 1000 simulated beams from the number of increments in the y -direction, therefore, it is recommended to use *ncuty* equal to the number of laminations. No difference was observed because PROLAM calculates apparent E from total deflection; therefore, the shear deflection did not affect the total deflection enough for significant differences to be observed.

Effect of Shear Deflection

In the next sensitivity analysis, the effect the shear deflection model has on the average apparent E is studied. Figure 6.1 is the fitted three-parameter lognormal probability distribution function (PDF) of the apparent E for the different shear deflection prediction methods.

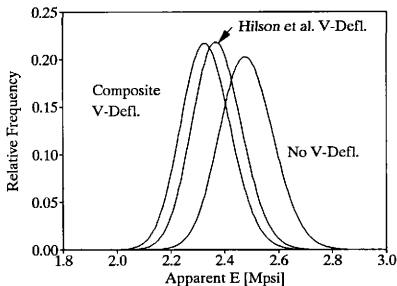


Figure 6.1: Comparison between different shear prediction methods.

Once again, the random number seed was held constant and E/G was equal to 16 for the three different simulations. As expected, the PDF for no shear deflection was furthest to the right of the three PDF's. By adding an approximate shear deflection model (Hilson, et al. 1988) to PROLAM, the PDF was shifted to the left. By adding the more accurate composite shear deflection model, the PDF was shifted even further to the left. The statistical calculations for the three test scenarios are summarized in Table 6.3. The fitted PDF's were plotted instead of the histograms to make the plot readable and differences between the methods could be observed easier. A sample size of 1000 beams was used in this case study.

Table 6.3: Effect of shear deflection model on apparent modulus of elasticity.

Shear Deflection Model	Modulus of Elasticity*	
	Average (Mpsi)	COV† (%)
no shear deflection	2.484	4.0
Hilson et al.	2.374	3.9
composite	2.333	4.0

* Predicted using PROLAM

† Coefficient of variation

The ratio of the apparent E with shear deflection included to the apparent E without shear deflection is 0.94. This is very similar to the 0.95 factor found in ASTM D3737 (ASTM, 1991e) that reduces the calculated E values for glulam beams. This standard specifically states that the 0.95 factor accounts for shear deflection.

Effect of E/G Ratio

The effect of the E/G ratio on PROLAM using the composite beam analysis is presented next. As discussed in Chapter V, a computer simulation was performed with an $E/G = 20$ for all lumber grades except L3, where $E/G = 30$. Figure 6.2 illustrates the PDF for this computer simulation with the PDF from the previous case study for the composite shear deflection model overlaid on the plot.

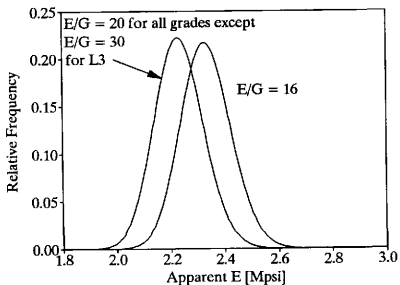


Figure 6.2: Effect of different E/G ratios on apparent E .

Figure 6.2 indicates that the E/G for the individual lumber grades has a pronounced effect on the apparent E predicted by PROLAM. The average E was 2.234 Mpsi with a coefficient of variation (COV) of 4.0%. This COV was identical to the case where E/G was equal to 16; however, the mean was reduced by approximately 100 000 psi.

Effect of L/d on Design Equations for Deflection

PROLAM was developed as a tool to analyze different case scenarios without having to destructively test glulam beams. An L/d ratio of 20 gives beam E corresponding to the book value used by designers. A case study was conducted using PROLAM for three different loading scenarios: 1) two-point loading (load span equal to 20% of total span), 2) a uniform loading and 3) single-point loading at the midspan. These simulations were performed with an $E/G = 16$ and then repeated for an $E/G = 20$ for all lumber grades except L3 where $E/G = 30$. The E for the first run at $L/d = 20$ was used as the design E for the beam layout, which in this case was a 24F-V4 Douglas-fir beam. The

deflections for the three different loading cases, and the two E/G studies were calculated at L/d ratios of 8, 10, 12.5, 15, 20, 25, 30 and 35 using the common design equations given as Equations 6.1, 6.2 and 6.3. The sample size was 1000 beams for all loading scenarios and the Δx was set equal to 6 in. The actual deflection of the beams were estimated by taking the average apparent E from PROLAM and back-solving for deflection using the appropriate beam equation. The deflection equation for two-point is as follows:

$$\delta = \frac{Pa}{48EI} (3L^2 - 4a^2) \quad (6.1)$$

Equation 6.2 is the deflection equation for uniformly loaded members.

$$\delta = \frac{5}{384} \frac{wL^4}{EI} \quad (6.2)$$

Equation 6.3 represents the deflection equation for a single concentrated load at midspan.

$$\delta = \frac{PL^3}{48EI} \quad (6.3)$$

Figures 6.3, 6.4 and 6.5 represent the error in the predicted deflection for the various L/d ratios for the three loading conditions.

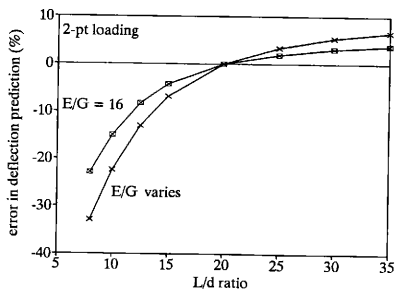


Figure 6.3: Error in predicted deflections for different L/d ratios for a two-point symmetric load.

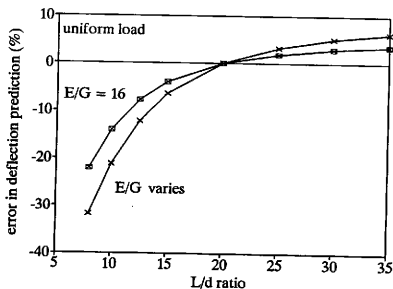


Figure 6.4: Error in predicted deflections for different L/d ratios for a uniform load.

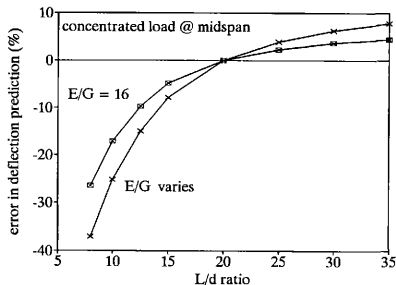


Figure 6.5: Error in predicted deflections for different L/d ratios for a concentrated load at midspan.

The effect that E/G ratio has on the error of the prediction can be seen in Figures 6.3, 6.4 and 6.5. The graphs all have similar characteristics. For long spans (L/d greater than 20) where deflection could control the design, the deflections using Equations 6.1, 6.2 and 6.3 are larger than the actual deflections predicted by PROLAM. For wood beams with an L/d ratio in the range of 15 to 25, Equation 6.1, 6.2 and 6.3 are commonly considered sufficiently accurate (Hoyle and Woeste, 1989). However, the results shown in Figures 6.3, 6.4 and 6.5 indicate errors of approximately 10% for L/d of 15, which may not be acceptable.

SUMMARY

The composite shear deflection model developed in Chapter III was implemented in an existing glued-laminated timber beam model called PROLAM. The sensitivity that several parameters had on the apparent E predicted from PROLAM were analyzed. The

number of increments along the length and depth of the beam had little effect on the apparent E predicted by PROLAM. Recommended values for Δx are whole numbers which correspond to the locations of point loads. A Δx of either 12 in. or 6 in. was chosen for all the case studies performed. The recommended number for $ncuty$ is the same as the number of laminations in the beam.

The E/G ratio had a significant effect on the apparent E predictions, therefore the E/G ratio is an important parameter and future research is needed to better characterize the shear modulus. The common engineering design practice of ignoring shear deflection for L/d ratios of 15 to 25 can lead to significant error, depending on the loading condition and the E/G ratio.

CHAPTER VII

SUMMARY AND CONCLUSIONS

SUMMARY

Beam deflection due to flexure is comprised of two components: 1) bending and 2) shear deflection. Shear deflection for many structural materials is ignored; however, wood has a relatively low shear stiffness as compared to bending stiffness. Shear deflection for wood beams can exceed the bending deflection under certain situations; therefore, it should be considered. This problem is reasonably straightforward for solid sawn lumber; however, it becomes more complex for composite beams such as glued-laminated timber beams and I-beams.

There are several possible methods to develop a shear deflection model for composite beams. A popular method that often is used in beam mechanics is the finite element (FE) method; however, this requires complex input that is neither completely understood for wood nor characterized for the multitude of wood species groupings. Using a FE method for wood can create a false sense of accuracy since these methods are only as accurate as the input parameters. Hence, a method was derived that was less computationally rigorous, and requires less input parameters.

The shear deflection equation developed here was based on energy methods and an extension of basic mechanics of materials. During development of the shear deflection model, an intermediate step was the development of an equation that characterizes the shear stress distribution for composite beams. A possible application of the shear stress equation would be to use it in a probabilistic model to predict shear strength of composite beams. Although several researchers have developed methods to predict shear deflection, they are not general enough to handle composite glulam beams, I-beams and nonprismatic

shapes. Another advantage of the composite shear deflection model is its ability to analyze G as a stochastic variable.

The composite shear deflection finite difference model was verified by comparing it to both theory and to published shear deflection models. The model performed well in all cases studied. The model was also compared to a set of actual glulam beams that were fabricated by AITC and tested by the U.S. Forest Products Laboratory. The comparison was made between the predicted apparent E of the beam by using individual E profiles of lumber that comprises the glulam beam to actual measured beam E . The difference in the actual beam E and predicted E was less than two percent. A paired t-test indicated a *statistically* significant difference between predicted and observed means; however, the low variability in the E data made it easy to reject the null hypothesis that the two average E 's were identical. The difference between predicted and actual apparent E was believed to be caused by a regression equation that related \bar{E}_{CLT} to \bar{E}_s , not the composite shear deflection model.

The composite shear deflection model was incorporated into an existing glulam beam model and sensitivity studies were performed. It was found that the number of increments along the length and depth for the finite difference model had little effect on the prediction capabilities of the model. It is recommended that the number of increments in the y -direction (beam depth) be equal to the number of laminations for a glulam beam. It is recommended that the number of increments in the x -direction (beam length) be chosen so an increment will correspond to the location of a concentrated load for greater accuracy. It is also recommended that the number of increments along the length of the beam be at least 25.

A sensitivity analysis was performed to determine the effect of the E/G ratio. This ratio is often assumed to be 16 for Douglas-fir lumber; however, several researchers indicate G is a random variable, not perfectly correlated to E . A significant effect was seen when the E/G ratio was set equal to 20 for all lumber grades except L3, which it was set equal

to 30, for the 24F-V4 beam combination. This affected the apparent beam E by approximately 100 000 psi.

An important finding was that the common engineering design practice of ignoring shear deflection for L/d ratios between 15 to 25 can lead to significant errors. Underconservative errors of approximately 10% were observed for a composite glulam beam at an L/d ratio of 15 for a concentrated load at midspan. This case was assuming the E/G ratio equaled 20 for all lumber grades except L3, where it was assumed to be equal to 30.

CONCLUSIONS

The following conclusions were made as a result of this research:

1. Shear deflection is significant for wood beams, especially for composite beams.
2. A finite difference solution to predict shear deflection for composite beams gives excellent results as compared to theory as well as other shear deflection models.
3. A finite difference solution that includes shear deflection to predict apparent E for composite glulam beams gives reasonable results as compared to actual test data.
4. The regression equation relating E_{CLT} and E_s has a significant impact on the models prediction capability; therefore, it should be periodically updated.
5. The E/G ratio has a significant effect on the shear deflection predictions. More research is needed to characterize localized shear modulus.
6. The number of increments along the length and depth of the beam for the finite difference model has little effect on the models prediction capability. It is recommended to use a $\Delta x = 12$ in. and a Δy equal to the number of laminations of the beam.
7. The common engineering design practice of ignoring shear deflection for L/d ratios between 15 and 25 can lead to significant errors for composite glulam beams.

8. Average two-ft static bending E measured was higher than long-span E . The two-ft E was collected under "third-point" loading with the shear-free E being collected between the load heads. The long-span E was collected at an L/d ratio equal to 100 to minimize the effects of shear deflection. More research is needed to characterize the relationship between short-span and long-span E .

RECOMMENDATIONS FOR FURTHER RESEARCH

The following areas were identified as candidates for further research:

1. Study the spatial variation of G , as well as its relationship to other material properties.
2. Develop a stochastic model that accurately and independently predicts G .
3. Investigate the apparent discrepancy between two-ft static bending shear-free E and long-span E .
4. Incorporate the composite shear stress equation into PROLAM to predict design shear stresses.
5. Validate the shear deflection model for composite I-beams using actual test data.
6. Develop a probabilistic model similar to PROLAM for wood I-beams.

REFERENCES

- Allen D.H. and W.E. Haisler. 1985. Introduction to aerospace structural analysis, John Wiley and Sons, New York. 507 pp.
- American Institute of Timber Construction (AITC). 1990. Modulus of elasticity of E-rated lumber by static loading. AITC 200-90 Inspection Manual. AITC, Vancouver, WA.
- . 1988. Standard specifications for structural glued-laminated timber of softwood species. AITC 117-Manufacturing. AITC, Vancouver, WA.
- American Society for Testing and Materials (ASTM). 1991a. Standard methods of static tests of timbers in structural sizes. ASTM Standard D198-84. ASTM, Philadelphia, PA.
- . 1991b. Standard practice for establishing structural grades and related allowable properties for visually graded lumber. ASTM Standard D245-88. ASTM, Philadelphia, PA.
- . 1991c. Standard practice for evaluating allowable properties for grades of structural lumber. ASTM Standard D2915-90. ASTM, Philadelphia, PA.
- . 1991d. Standard test method for shear modulus of plywood. ASTM Standard D3044-88. ASTM, Philadelphia, PA.
- . 1991e. Standard test method for establishing stresses for structural glued laminated timber (glulam). ASTM Standard D3737-89a. ASTM, Philadelphia, PA.
- . 1991f. Standard test methods for mechanical properties of lumber and wood-based structural material. ASTM Standard D4761-88. ASTM, Philadelphia, PA.
- Baird, J.A. and E.C. Ozelton. 1984. Timber designers' handbook, Granada Publishing Ltd, London. 624 pp.
- Bender, D.A. 1990. Correspondence to R. Hernandez, August 30.
- Biblis, E.J. 1965. Shear deflection of wood beams. Forest Prod. J. 15(11):492-498.
- Bodig J. and J.R. Goodman. 1973. Prediction of elastic parameters for wood. Wood Science 5(4):249-264.

- _____. and B.A. Jayne. 1982. Mechanics of wood and wood composites, Van Nostrand Reinhold Co, New York. 712 pp.
- Boresi, A.P. and O.M. Sidebottom. 1985. Advanced mechanics of materials, 4th ed., John Wiley and Sons, New York. 763 pp.
- Bradtmueller, J.P., M.O. Hunt and K.J. Fridley. 1991. Factors influencing the Purdue shear modulus bending test for wood composites. Presented at 45th annual meeting. Forest Prod. Res. Soc., New Orleans, LA.
- Chapra, S.C. and R.P. Canale. 1988. Numerical methods for engineers, 2nd ed., McGraw-Hill Book Company, New York. 812 pp.
- Chui, Y.H. 1991. Simultaneous evaluation of bending and shear moduli of wood and the influence of knots on these parameters. Wood Science and Technology 25:125-134.
- Commission of the European Communities. 1987. Eurocode 5: common unified rules for timber structures. Report No. EUR 9887 EN. CEC, Brussels.
- Davalos, J.F., J.R. Loferski, S.M. Holzer and V. Yadama. 1991. Transverse isotropy modeling of 3-D glulam timber beams. Journal of Materials in Civil Engineering 3(2):125-139.
- Doyle, D.V. 1968. Properties of no. 2 dense kiln-dried southern pine dimension lumber. Res. Paper FPL 96. U.S. Department of Agriculture, Forest Service, Forest Prod. Lab., Madison, WI.
- _____. and L.J. Markwardt. 1966. Properties of southern pine in relation to strength grading of dimension lumber. Res. Paper FPL 64. U.S. Department of Agriculture, Forest Service, Forest Prod. Lab., Madison, WI.
- _____. and _____. 1967. Tension parallel-to-grain properties of southern pine dimension lumber. Res. Paper FPL 84. U.S. Department of Agriculture, Forest Service, Forest Prod. Lab., Madison, WI.
- Ebrahimi, G. and A. Sliker. 1981. Measurement of shear modulus in wood by a tension test. Wood Science 13(3):171-176.
- Gere, J.M. and S.P. Timoshenko. 1984. Mechanics of materials, 2nd ed., Wadsworth, Belmont, CA. 762 pp.
- Goodman, J.R. and J.Bodig. 1978. Contemporary methods for modelling the elastic behavior of wood. In Proc. general constitutive relations for wood and wood-based materials, 17-45. The National Science Foundations, Syracuse, NY.

- Gunnerson, R.A., J.R. Goodman and J. Bodig. 1973. Plate tests for determination of elastic parameters of wood. *Wood Science* 5(4):241-248.
- Hernandez, R. 1991. Simulation modeling and analysis of glued-laminated timber beams. M.S. thesis, Department of Agricultural Engineering, Texas A&M University, College Station, TX.
- , D.A. Bender, B.A. Richburg and K.S. Kline. (in press). Probabilistic modeling of glued-laminated timber beams. *Wood and Fiber Science*.
- Hilson, B.O, L.R.J. Whale and P.D. Rodd. 1990. The deflection of glued-laminated timber beams. *Journal Institute of Wood Science* 12(2):67-70.
- , P.J. Pellicane, L.R.J. Whale and I. Smith. 1988. Towards optimal design of glued-laminated timber beams. *In Proc. international conference on timber engineering*, ed. R. Y. Itani, II:186-193. Forest Prod. Res. Soc., Seattle, WA.
- Hoyle, R.J. and F.E. Woeste. 1989. *Wood technology in the design of structures*, 5th ed., Iowa State University Press, Ames, IA. 394 pp.
- Hsu, T.T.C. 1984. *Torsion of reinforced concrete*, Van Nostrand Reinhold, New York. 516 pp.
- Law, A.M. and W.D. Kelton. 1991. *Simulation modeling and analysis*, 2nd ed., McGraw-Hill Book Company, New York. 400 pp.
- Kline, D.E., F.E. Woeste, and B.A. Bendtsen. 1986. Stochastic model for modulus of elasticity of lumber. *Wood and Fiber Science* 18(2): 228-238.
- Mansour, M.H. and V.K.A. Gopu. 1990. Statistical analysis of pitch-cambered beam deflections due to moe variability. *In Proc. international conference on timber engineering*, ed. H. Sugiyama, I:170-175. Forest Prod. Res. Soc., Tokyo, Japan.
- National Design Specifications (NDS). 1986. National Forest Prod. Association, Washington, D.C.
- Orosz, I. 1970. Simplified method for calculating shear deflection of beams. Res. Note FPL 210. U.S. Department of Agriculture, Forest Service, Forest Prod. Lab., Madison, WI.
- Palka, L.C. and J.D. Barrett. 1985. An examination of E/G values for canadian spruce lumber. Report to ASTM task group investigating the validity of Table 2 of ASTM D 2915-74. Forintek Canada Corp. Report on file at ASTM headquarters.

- Pellicane, P.J. and B.O. Hilson. 1985. A computer model to predict the elastic response of composite beams with inhomogeneous lamella. Brighton Polytechnic report to the Timber Research and Development Association, United Kingdom.
- Richburg, B.A. 1989. Modeling localized properties of E-rated laminating lumber. M.S. thesis, Department of Agricultural Engineering, Texas A&M University, College Station, TX.
- Salmon C.G. and J.E. Johnson. 1990. Steel structures: design and behavior - emphasizing load and resistance factor design, 3rd ed., Harper & Row, Publishers, New York. 1086 pp.
- Shigley J.E. and L.D. Mitchell. 1983. Mechanical engineering design, 4th ed., McGraw-Hill Book Company, New York, NY. 869 pp.
- Swift, G.W. and R.A. Heller. 1974. Layered beam analysis. Journal of Engineering Mechanics Division of the American Society of Civil Engineers (ASCE) 100(EM2):267-282.
- Taylor, S.E. 1988. Modeling spatial variability of localized lumber properties. Ph.D. Dissertation, Department of Agricultural Engineering, Texas A&M University, College Station, TX.
- USDA. 1987. Wood handbook: wood as an engineering material. Agric. Handb. 72. U.S. Department of Agriculture, Forest Service, Forest Prod. Lab., Madison, WI.
- Walpole R.E. and R.H. Myers. 1978. Probability and statistics for engineers and scientists, 2nd ed., Macmillan Publishing Company, New York. 580 pp.
- Wangaard, F.F. 1964. Elastic deflection of wood-fiberglass composite beams. Forest Prod. J. 14(6):256-260.
- Zhang, W. and A. Sliker. 1991. Measuring shear moduli in wood with small tension and compression samples. Wood and Fiber Science 23(1):58-68.

APPENDIX A**COMPOSITE BEAM DEFLECTION MODEL FORTRAN CODE**

```

=====
c
c This program calculates the deflection for a composite beam
c with varying widths and shapes. For more information see:
c
c Hilson, B.O.,P.J. Pellicane, L.R.J. Whale and J. Smith.
c 1988. Towards optimal design of glued-laminated timber
c beams. In Proc. international conference on timber
c engineering, ed. R.Y. Itani, II:186-193. Seattle, WA:
c Forest Products Research Society.
c
c Skaggs, T.D. 1992. Shear deflection of composite wood
c beams. M.S. Thesis, Department of Agricultural Engineering,
c Texas A&M University, College Station, TX.
c
c Written by: Thomas D. Skaggs
c November 1991
c
=====
c
c VARIABLE LIST
c
c addupm = used to sum deflection due to bending
c addupv = used to sum deflection due to shear
c b(i) = width of the i-th lamination
c def = total deflection due to bending and shear
c delta = increment for model along the length of the beam
c depth = depth of beam
c e(i) = modulus of elasticity of the i-th lamination
c e15 = arbitrary value for E to transform the cross section
c to (1.5e6 psi)
c itran = moment of inertia calculated for the transformed
c cross section
c lbeam = length of the beam
c midspn = distance from the end to the center of the beam
c mx = theoretical moment at the x-section being checked
c mxunit = theoretical moment caused by a unit load at midspan
c ncutex = number of cuts along the length of the beam
c ncuty = number of cuts per lamination in the y-direction
c nlims = number of laminations in the cross section
c p = arbitrary load used to calculate deflection from a
c symmetric two-point load
c q = first moment of inertia
c r1 = reaction for one side for uniform loading
c t = thickness of the laminations
c tcut = thickness of the cut in the y-direction
c tload = type of load on beam
c 1 = uniform load
c 2 = symmetric 2-point loading
c vx = theoretical shear at the x-section being checked
c vxunit = theoretical shear caused by a unit load at midspan
c w = arbitrary load used to calculate deflection from a
c uniform load
c x = location where cross section is being checked
c xx = location where cross section is being checked
c x1 = distance from end of beam to first load for
c symmetric 2-pt loading
c x2 = distance from end of beam to second load for
c symmetric 2-pt loading
c ybar = distance from bottom of beam to centroid
c
c TEMPORARY TERMS
c
c a = temporary term used to calculate ybar and itran
c ay = temporary summation variable used to calculate ybar
c suma = temporary summation variable used to calculate ybar
c sumq = temporary summation variable used to calculate deflection
c sumy = temporary summation variable used to calculate deflection
c
=====
c
c program deflect
c real itran,b(50),e(50),lbeam,midspn,mx,mxunit
c open (unit=10,file='deflect.inp',status='old')
c open (unit=20,file='deflect.out',status='unknown')

```

```

c-> format statements
10 format (/,/,/,/,
+   12x, '*****',
+   12x, '*****'
20 format (/,/,/,/,
+   12x, '*****',
+   12x, '*****'
30 format (/,/,/,/,
+   12x, '*****',
+   12x, '*****'
40 format (12x, '*****')
50 format (12x, '*****')
60 format (12x, '*****')
70 format (12x, '*****')
80 format (12x, '*****')
110 format (12x, '*****')
+   12x, '*****',
+   12x, '*****',
+   12x, '*****',
120 format (12x, '*****')
130 format (12x, '*****')
140 format (12x, '*****')
150 format (12x, '*****')
160 format (12x, '*****')
c-> initialize variables
w = 10
p = 1000
e15 = 1.5e6
ncuty = 1
c-> read input from DEFLECT.INP
read (10,*) tload
if (tload.eq.1) read(10,*) w
if (tload.eq.2) read(10,*) p
read (10,*) n1lms,t,lbeam,x1,delta
read (10,*) (b(i),e(i),i=1,n1lms)
if (tload.eq.2) then
  if (x1.gt.lbeam/2.0) then
    write (20,10)
    goto 500
  endif
endif
if (tload.eq.1) write (20,20)
if (tload.eq.2) write (20,30)
write (20,40)
write (20,50) lbeam,t
if (tload.eq.1) write (20,60) w
if (tload.eq.2) write (20,70) P/2.,x1
write (20,40)
write (20,80)
write (20,40)
depth = 0
suma = 0.
ay = 0.
c-> calculate distance to the centroid
do 200 i=1,n1lms
  depth = depth+t
  a = b(i)*t*e(i)/e15
  suma = suma+a
200  ay = ay+a*(depth-t/2.)
ybar = ay/suma
depth = 0.
itrans = 0.
c-> calculate I for the transformed cross section
do 210 i=1,n1lms
  depth = depth+t
  a = b(i)*t*e(i)/e15
210  itrans = itrans+a*t*t/12.+a*(ybar-depth+t/2.)**2
lbeam = lbeam*12.
midspn = lbeam/2.
x1 = x1*12.
x2 = lbeam-x1
rl = w*lbeam/2.

```

```

ncutx = int((beam/delta)
addupm = 0.0
addupv = 0.0
c-> calculate theoretical shear and moment distributions
do 240 i=1,ncutx
  x = delta*real(i-1)
  if (x.le.midspn) then
    mxunit = 0.5*x
    vxunit = 0.5
  else
    mxunit = 0.5*(beam-x)
    vxunit = -0.5
  endif
  if (tload.eq.1) then
    vx = r1 - w*x
    mx = r1*x - w*x*x/2.
  else
    xx = x
    mx = p/2.*x1
    vx = 0.0
    if (xx.gt.x2) xx = lbeam - xx
    if (xx.le.x1) then
      mx = p/2.*xx
      vx = p/2.
    endif
    if (x.gt.x2) vx = -p/2.
  endif
  depth = 0.0
  q = 0.0
  sumq = 0.0
  sumy = 0.0
c-> calculate shear deflection (Skaggs, 1992)
do 220 j=1,nlams
  tcut = t/real(ncuty)
  do 220 k=1,ncuty
    depth = depth+tcut
    q = b(j)*tcut*(ybar-depth+tcut/2.)
    sumq = sumq + e(j)*q/e15
  220  sumy = sumy + tcut*sumq*sumq/(e(j)*b(j))
  addupv = addupv+(delta*sumy*16.*vx*vxunit)/
  + (itran*itran)
c-> calculate bending deflection (Hilson et al., 1988)
240  addupm = addupm+mx*mxunit*delta/(e15*itran)
  def = addupv+addupm
c-> write output to DEFLECT.OUT
write (20,110)b(1),e(1)/1.e6
write (20,120)(i,b(i),e(i)/1.e6,i=2,nlams-1)
write (20,130)nlams,b(nlams),e(nlams)/1.e6
write (20,40)
write (20,80)
write (20,40)
write (20,150)
write (20,40)
write (20,140) addupm,addupv
write (20,160) def
write (20,40)
write (20,80)
close (unit=10)
close (unit=20)
500 stop
end

```

APPENDIX B**OROSZ'S (1970) FORM FACTOR QUATTRO PRO CODE**

A1: This worksheet calculates k for the shear deflection equation.
 A2: It was originally derived for an I-beam, but possible applications
 A3: could be a glulam beam with 2 different lumber grades. It should
 A4: be noted that it is only valid for a beam that is symmetric about
 A5: the neutral axis.
 A7: Ref: Orosz, I. 1970. Simplified method for calculating shear
 A8: deflections of beams. U.S.D.A. Forest Service Research Note FPL-210,
 A9: U.S. Forest Products Laboratory, Madison, WI.
 E13: "p =
 F13: 500
 B14: "Beta =
 C14: 1
 E14: "a =
 F14: 84
 B15: "p =
 C15: (3/8)/(3*2.25)
 E15: "A =
 F15: 24.375
 B16: "t =
 C16: 11/14
 E16: "E =
 F16: 1000000
 A19: "a1 =
 B19: ((1-T)/SP+T)
 A20: "a2 =
 B20: (T^5/2-T^3+T/2)/SP^2
 A21: "a3 =
 B21: ((-T^5)*(1/(10*BETA)+2/3)+T^3*(1/(3*BETA)+2/3)-T/(2*BETA)+8/(30*BETA))/SP
 D21: "k =
 E21: 4.5*B*19*(B\$20+B\$21+B\$22)/B\$24
 A22: "a4 =
 B22: 8*T^5/30
 A24: "b1 =
 B24: ((1-T^3)/SP+T^3)^2
 A F15
 BETA C14
 E F16
 K E21
 P C15
 T C16

APPENDIX C**MANSOUR AND GOPU'S (1990) FORM FACTOR FORTRAN CODE**

```

=====
c
c This program calculates the form factor used to calculate
c shear deflection for rectangular composite beams.
c Adapted from:
c
c Mansour, M.H. and V.K.A. Gopu. 1990. Statistical analysis
c of pitch-cambered beam deflections due to MOE variability.
c In Proc. international conference on timber engineering,
c ed. H. Sugiama, 1:170-175. Tokyo, Japan: Forest
c Products Research Society.
c
c Written by: Thomas D. Skaggs
c November 1991
c
=====
c
c VARIABLE LIST
c
c atran = area of the transformed section
c b(i) = transformed width of the i-th lamination
c base = width of the cross section
c c(i) = term used to calculate k, Equation 11 (Mansour
c and Gopu, 1990)
c e(i) = modulus of elasticity of the i-th lamination
c ebar = average E for the cross section
c itran = moment of inertia calculated for the transformed
c cross section
c k = form factor used to calculate shear deflection
c for composite rectangular beams.
c nlams = number of laminations in the cross section
c t = thickness of the laminations
c y(i) = distance from the bottom fiber of the cross
c section to the top fibers of the i-th lamination
c ybar = distance from bottom of beam to centroid
c
c TEMPORARY TERMS
c
c a1 = temporary term used to calculate k
c b2 = temporary term used to calculate k
c c3 = temporary term used to calculate k
c sum1 = temporary summation variable
c sum2 = temporary summation variable
c
=====
program mansour
real b(50),c(50),y(51),e(50),itran,k
open (unit=10,file='mansour.inp',status='old')
open (unit=20,file='mansour.out',status='unknown')
c-> format statements
10 format (12x, '=====> MANSOUR.OUT <=====')
20 format (12x, '45x')
30 format (12x, ' Thickness of laminations (in) : 'f6.3' '//,
+ 12x, ' Width of laminations (in) : 'f6.3' '//,

40 format (12x, '=====>')
50 format (12x, ' Lam MOE '//,
+ 12x, ' (Mpsi) '//,
+ 12x, '45x' '//,
+ 12x, '1(C)'12x, 'f6.3,11x'')
60 format (12x, '12,15xf6.3,11x'')
70 format (12x, '12, '(T)'12x, 'f6.3,11x, '1')
80 format (12x, '45x' '//,
+ 12x, ' Average E of lams (Mpsi) : 'f8.3' '//,
+ 12x, ' Transformed I (in^4) : 'f8.3' '//,
+ 12x, ' Form factor (k) : 'f8.6' '//,

c-> read input from MANSOUR.INP
read(10,*) nlams,t,base
read(10,*) (e(i),i=1,nlams)
sum1 = 0.0
y(1) = 0.0

c-> calculate average E for cross section
do 200 i=1,nlams
sum1 = sum1+e(i)

```



```

200  y(i+1) = t*real(i)
      ebar = sum1/real(nlams)
c-> transform the width of the i-th lamination
do 210 i=1,nlams
210  b(i) = base*e(i)/ebar
      sum1 = 0.0
      atran = 0.0
c-> calculate distance to the centroid
do 220 i=1,nlams
      sum1 = sum1 + b(i)*(y(i+1)+y(i+1)-y(i))*y(i))
220  atran = atran + b(i)*(y(i+1)-y(i))
      ybar = 0.5*sum1/attran
      sum1 = 0.0
      sum2 = 0.0
c-> calculate I for the transformed cross section
do 230 i=1,nlams
      sum1 = sum1 + b(i)*(y(i+1)-y(i))**3/12.
230  sum2 = sum2 + b(i)*(y(i+1)-y(i))*(y(i+1)+y(i)-2*ybar)**2
      itrans = sum1 + sum2/4.
      sum1 = 0.0
      sum2 = 0.0
c-> calculate k using Eq. 10 & 11 (Mansour and Gopu, 1990)
do 250 i=1,nlams
      c(i) = 0.0
do 240 j=i+1,nlams
240  c(i) = c(i)+b(j)*((y(j+1)-ybar)**2-(y(j)-ybar)**2)
      a1 = ((y(i+1)-ybar)-(y(i)-ybar))*((y(i+1)-ybar)**2+c(i))**2
      b2 = ((y(i+1)-ybar)**3-(y(i)-ybar)**3)*((y(i+1)-ybar)**2+c(i))
      c3 = ((y(i+1)-ybar)**5-(y(i)-ybar)**5)
      sum1 = sum1+b(i)*(y(i+1)-y(i))/(4.*itrans*itrans)
250  sum2 = sum2+b(i)*(a1-2.*b2/3.+c3/5.)
      k = sum1*sum2
c-> write output to MANSOUR.OUT
write (20,10)
write (20,20)
write (20,30) t,base
write (20,20)
write (20,40)
write (20,20)
write (20,50) e(1)/1.e6
write (20,60)(i,e(i)/1.e6,i=2,nlams-1)
write (20,70) nlams,e(nlams)/1.e6
write (20,20)
write (20,40)
write (20,80) ebar/1.e6,itrans,k
write (20,20)
write (20,40)
close (unit=10)
close (unit=20)
stop
end

```

APPENDIX D
BEAM E MODEL FROM CLT MAP FORTRAN CODE

```

=====
c
c This program calculates the apparent MOE values given the
c cit beam profiles.
c
c References:
c
c Hilsen, B.O.,P.J. Pellicane, L.R.J. Whale and I. Smith.
c 1988. Issues on optimal design of glued-laminated timber
c beams. In Proc. international conference on timber
c engineering, ed. R.Y. Itani, II:186-193. Seattle, WA:
c Forest Products Research Society.
c
c Skaggs, T.D. 1992. Shear deflection of composite wood
c beams. M.S. Thesis, Department of Agricultural Engineering,
c Texas A&M University, College Station, TX.
c
c          Written by: Thomas D. Skaggs
c                   November 1991
c
=====
c
c VARIABLE LIST
c
c bold      = special screen function, turns bold on
c comment   = character statement for comments
c data(i,j) = CLT-E data read in then transformed to static
c            bending E for the i-th segment and the j-th lam
c diff      = difference between actual and predicted E
c e(i)      = actual measured E for the i-th beam
c error     = percent error in prediction
c infile(i) = data file name for the i-th beam
c pe(i)     = predicted E for the i-th beam
c nbeam     = number of beams to analyze
c sum$      = summation terms for statistical calculations
c sum$2     = summation terms for statistical calculations
c t         = paired t-test statistic
c $bar      = average for the respective variable
c $var      = variance for the respective variable
c
=====
c
c program beame
c real data(40,16),e(30),pe(30)
c character*7 infile(30)
c nbeam = 29
c sume = 0.
c sume2 = 0.
c sumpe = 0.
c sumpe2 = 0.
c sumd = 0.
c sumd2 = 0.
c-> format statements
c 10 format (a7,2x,f5.3)
c 20 format (/10x,'infile'1x,2(6x'Beam-E'),8x,'diff'7x,
c    + 'error'1,23x,'actual'7x,'pred'22x,'%'/)
c 30 format (5x,a12,4(5x,f7.3))
c open (10,file='beame.inp',status='old')
c open (20,file='beame.out',status='new')
c-> read data filenames
c do 100 i=1,nbeam
c 100 read (10,10) infile(i), e(i)
c close (10)
c write (20,20)
c do 130 ii=1,nbeam
c open (11,file=infile(ii),status='old')
c-> read data from 'infile(11)'
c do 110 i=1,39
c 110 read (11,*) (data(i,j),j=1,16)
c close(11)
c-> transform CLT-E to Static Bending (Skaggs, 1992)
c do 120 i=1,39
c do 120 j=1,16
c 120 data(i,j)=1.0e6*(1.3224*data(i,j)-0.2344)
c data(i,j)=1.227*data(i,j)-0.191

```

```

c 120      data(i,j)=1.0e6*(1.142*data(i,j)-0.219)
120      data(i,j)=1.0e6*(1.227*data(i,j)-0.191)
      call trform(data,bnoe)
      pe(ii) = bnoe
      diff = pe(ii)-e(ii)
      error = 100*diff/e(ii)
      sune = sune + e(ii)
      sune2 = sune2 + e(ii)*e(ii)
      sumpe = sumpe + pe(ii)
      sumpe2 = sumpe2 + pe(ii)*pe(ii)
      sund = sund + diff
      sund2 = sund2 + diff*diff
130 write (20,30) infile(ii), e(ii), pe(ii), diff, error
c-> calculate statistical parameters
      ebar = sune/real(nbeam)
      pebar = sumpe/real(nbeam)
      dbar = sund/real(nbeam)
      evar = ((real(nbeam)*sune2)-(sune*sune))/
+ (real(nbeam)*(real(nbeam)-1.))
      pevar = ((real(nbeam)*sumpe2)-(sumpe*sumpe))/
+ (real(nbeam)*(real(nbeam)-1.))
      dvar = ((real(nbeam)*sund2)-(sund*sund))/
+ (real(nbeam)*(real(nbeam)-1.))
c-> calculate test statistic for paired t-test
      t = dbar/sqrt(dvar/real(nbeam))
      write (20,40) ebar,pebar,dbar,evar,pevar,dvar
40 format (/13x,'mean',3(5x,17.3),/,14x,'var',3(5x,17.3))
      write (20,50) t
50 format (/10x,'t-test statistic : ',f8.3)
      close (20)
      stop
      end
=====
c
c      =====
c      SUBROUTINE: TRFORM
c      =====
c
c VARIABLE LIST
c
c addupm = used to sum deflection due to bending
c addupv = used to sum deflection due to shear
c bnoe = apparent E of the beam
c b(i) = width of the i-th lamination
c def = total deflection due to bending and shear
c delta = increment for numerical integration along the
c length of the beam
c depth = depth of beam
c e(i,j) = static bending E for the i-th segment and j-th
c lamination
c e15 = arbitrary value for E to transform the cross section
c to (1.5e6 psi)
c gmod(j) = E/I ratio for the j-th lamination
c ig = gross moment of inertia
c i15 = moment of inertia calculated for the transformed
c cross section
c lbeam = length of the beam
c midspn = distance from the end to the center of the beam
c mx = theoretical moment at the x-section being checked
c mxunit = theoretical moment caused by a unit load at midspan
c ncuty = number of cuts per lamination in the y-direction
c nlam = number of laminations in the cross section
c p = arbitrary load used to calculate deflection from a
c symmetric two-point load
c q = first moment of inertia
c r1 = reaction for one side for uniform loading
c t = thickness of the laminations
c tcut = thickness of the cut in the y-direction
c vx = theoretical shear at the x-section being checked
c vxunit = theoretical shear caused by a unit load at midspan
c x = location where cross section is being checked
c xx = location where cross section is being checked
c x1 = distance from end of beam to first load for
c symmetric 2-pt loading

```

```

c  x2  = distance from end of beam to second load for
c      symmetric 2-pt loading
c  ybar = distance from bottom of beam to centroid
c
c  TEMPORARY TERMS
c
c  a    = temporary term used to calculate ybar and i15
c  ay   = temporary summation variable used to calculate ybar
c  suma = temporary summation variable used to calculate ybar
c  sumq = temporary summation variable used to calculate
c      shear deflection
c  sumy = temporary summation variable used to calculate
c      shear deflection
c
c=====
      subroutine trform(e,bmoec)
      real e(40,16),gmod(16),i15,lbeam,midspn,mx,mxunit,ig
c-> initialize variables
      data gmod /4*20.,8*30.,4*20./
      e15 = 1.5e6
      ncuty = 1
      nlms = 16
      t = 1.5
      base = 5.125
      delta = 12.0
      lbeam = 456.0
      x1 = 180.0
      x2 = 276.0
      midspn= 228.0
      p = 1000.
      ecdupv= 0.0
      eadupv= 0.0
      ig = 5904
      do 240 i=1,38
c-> calculate theoretical shear and moment distributions
      x = delta*real(i-1)
      if (x.le.midspn) then
        mxunit = 0.5*x
        vxunit = 0.5
      else
        mxunit = 0.5*(lbeam-x)
        vxunit = -0.5
      endif
      xx = x
      mx = p/2.*x1
      vx = 0.0
      if (xx.gt.x2) xx = lbeam - xx
      if (xx.le.x1) then
        mx = p/2.*xx
        vx = p/2.
      if (x.gt.x2) vx = -p/2.
      endif
      depth = 0.
      suma = 0.
      ay = 0.
c-> calculate distance to the centroid
      do 200 j=1,nlms
        depth = depth+t
        a = base*t*e(i,j)/e15
        suma = suma+a
      200  ay = ay+a*(depth-t/2.)
      ybar = ay/suma
      depth = 0.
      i15 = 0.
c-> calculate I for the transformed cross section
      do 210 j=1,nlms
        depth = depth+t
        a = base*t*e(i,j)/e15
      210  i15 = i15+a*t*t/12.+a*(ybar-depth+t/2.)**2
      depth = 0.0
      q = 0.0
      sumq = 0.0
      sumy = 0.0
c-> calculate shear deflection (Skaggs, 1992)

```

```

do 220 j=1,nlams
  tcut = t/real(ncuty)
  do 220 k=1,ncuty
    depth = depth+tcut
    q      = base*tcut*(ybar-depth+tcut/2.)
    sumq   = sumq + e(i,j)*q/e15
  220     sumy = sumy + tcut*sumq*sumq*gmod(j)/(e(i,j)*base)
    addupv = addupv+sumy*vx*vxunit*delta/(i15*i15)
c-> calculate bending deflection (Wilson et al., 1988)
  240     addupm = addupm+mx*mxunit*delta/(e15*i15)
    def = addupv+addupm
c-> backsolve for apparent MOE Eq. 4.2 (Skaggs, 1992)
    bmo = P*X1*{(3.0*(beam*lbeam)-(4.0*X1*X1))/
+          (1.0e6*48.0*def*lg)}
  return
end

```

APPENDIX E
E DATA FOR 24F-V4 GLULAM BEAMS

=====

AITC Project 8704R: Phase II Douglas-fir Glulam Beams

=====

E/G = 16
Using Equation 5.1 for the E-transformation

Beam ID	Actual E (Mpsi)	Pred E (Mpsi)	diff (Mpsi)	error (%)
B1	2.143	2.250	0.107	4.993
B2	1.943	2.106	0.163	8.389
B3	1.958	2.111	0.153	7.814
B4	2.085	2.187	0.102	4.892
B5	2.216	2.311	0.095	4.287
B6	2.136	2.204	0.068	3.184
B7	2.034	2.156	0.122	5.998
B8	2.094	2.161	0.067	3.200
B9	2.127	2.240	0.113	5.313
B10	2.072	2.166	0.094	4.537
R1	1.904	2.120	0.216	11.345
R2	2.072	2.278	0.206	9.942
R3	2.056	2.339	0.283	13.765
R4	2.105	2.250	0.145	6.888
R5	2.082	2.315	0.233	11.191
R6	1.843	2.085	0.242	13.131
R7	2.054	2.175	0.121	5.891
R8	2.057	2.196	0.139	6.757
R9	2.203	2.396	0.193	8.761
R10	2.038	2.204	0.166	8.145
T1	2.022	2.226	0.204	10.089
T2	2.163	2.283	0.120	5.548
T3	2.056	---	---	---
T4	2.145	2.384	0.239	11.142
T5	2.056	2.338	0.282	13.716
T6	2.075	2.251	0.176	8.482
T7	2.012	2.190	0.178	8.847
T8	2.062	2.264	0.202	9.796
T9	2.120	2.263	0.143	6.745
T10	1.956	2.296	0.340	17.382
avg	2.0632	2.2326	0.1694	8.2817
sd	0.0843	0.0818	0.0677	3.4799
COV(%)	4.0881	3.6649		

paired t-test statistic = 13.466

=====

AITC Project 8704R: Phase II Douglas-fir Glulam Beams

=====

E/G = 20 for all lams except L3 where E/G = 30
 Using Equation 5.1 for the E-transformation

Beam ID	Actual E (Mpsi)	Pred E (Mpsi)	diff (Mpsi)	error (%)
B1	2.143	2.168	0.025	1.167
B2	1.943	2.033	0.090	4.632
B3	1.958	2.039	0.081	4.137
B4	2.085	2.110	0.025	1.199
B5	2.216	2.227	0.011	0.496
B6	2.136	2.127	-0.009	-0.421
B7	2.034	2.080	0.046	2.262
B8	2.094	2.085	-0.009	-0.430
B9	2.127	2.160	0.033	1.551
B10	2.072	2.091	0.019	0.917
R1	1.904	2.048	0.144	7.563
R2	2.072	2.195	0.123	5.936
R3	2.056	2.252	0.196	9.533
R4	2.105	2.169	0.064	3.040
R5	2.082	2.231	0.149	7.157
R6	1.843	2.015	0.172	9.333
R7	2.054	2.100	0.046	2.240
R8	2.057	2.120	0.063	3.063
R9	2.203	2.306	0.103	4.675
R10	2.038	2.126	0.088	4.318
T1	2.022	2.146	0.124	6.133
T2	2.163	2.200	0.037	1.711
T3	2.056	---	---	---
T4	2.145	2.295	0.150	6.993
T5	2.056	2.251	0.195	9.484
T6	2.075	2.170	0.095	4.578
T7	2.012	2.113	0.101	5.020
T8	2.062	2.183	0.121	5.868
T9	2.120	2.181	0.061	2.877
T10	1.956	2.213	0.257	13.139
avg	2.0632	2.1529	0.0897	4.4197
sd	0.0843	0.0767	0.0660	3.3303
COV(%)	4.0881	3.5622		

paired t-test statistic = 7.318

=====

AITC Project 8704R: Phase II Douglas-fir Glulam Beams

=====

E/G = 16				
Using Equations 5.2 & 5.3 for the E-transformation				
Beam ID	Actual E (Mpsi)	Pred E (Mpsi)	diff (Mpsi)	error (%)
B1	2.143	2.202	0.059	2.753
B2	1.943	2.050	0.107	5.507
B3	1.958	2.056	0.098	5.005
B4	2.085	2.136	0.051	2.446
B5	2.216	2.268	0.052	2.347
B6	2.136	2.154	0.018	0.843
B7	2.034	2.103	0.069	3.392
B8	2.094	2.107	0.013	0.621
B9	2.127	2.193	0.066	3.103
B10	2.072	2.114	0.042	2.027
R1	1.904	2.065	0.161	8.456
R2	2.072	2.232	0.160	7.722
R3	2.056	2.297	0.241	11.722
R4	2.105	2.203	0.098	4.656
R5	2.082	2.272	0.190	9.126
R6	1.843	2.028	0.185	10.038
R7	2.054	2.124	0.070	3.408
R8	2.057	2.146	0.089	4.327
R9	2.203	2.358	0.155	7.036
R10	2.038	2.154	0.116	5.692
T1	2.022	2.177	0.155	7.666
T2	2.163	2.238	0.075	3.467
T3	2.056	---	---	---
T4	2.145	2.344	0.199	9.277
T5	2.056	2.296	0.240	11.673
T6	2.075	2.204	0.129	6.217
T7	2.012	2.139	0.127	6.312
T8	2.062	2.218	0.156	7.565
T9	2.120	2.216	0.096	4.528
T10	1.956	2.250	0.294	15.031
avg	2.0632	2.1843	0.1211	5.9297
sd	0.0843	0.0867	0.0696	3.4993
COV(%)	4.0881	3.9682		

paired t-test statistic = 9.369

=====

AITC Project 8704R; Phase II Douglas-fir Glulam Beams

=====

E/G = 20 for all lams except L3 where E/G = 30
 Using Equations 5.2 & 5.3 for the E-transformation

Beam ID	Actual E (Mpsi)	Pred E (Mpsi)	diff (Mpsi)	error (%)
B1	2.143	2.121	-0.022	-1.027
B2	1.943	1.979	0.036	1.853
B3	1.958	1.985	0.027	1.379
B4	2.085	2.060	-0.025	-1.199
B5	2.216	2.183	-0.033	-1.489
B6	2.136	2.078	-0.058	-2.715
B7	2.034	2.028	-0.006	-0.295
B8	2.094	2.032	-0.062	-2.961
B9	2.127	2.113	-0.014	-0.658
B10	2.072	2.040	-0.032	-1.544
R1	1.904	1.995	0.091	4.779
R2	2.072	2.150	0.078	3.764
R3	2.056	2.210	0.154	7.490
R4	2.105	2.123	0.018	0.855
R5	2.082	2.188	0.106	5.091
R6	1.843	1.959	0.116	6.294
R7	2.054	2.050	-0.004	-0.195
R8	2.057	2.071	0.014	0.681
R9	2.203	2.268	0.065	2.951
R10	2.038	2.077	0.039	1.914
T1	2.022	2.097	0.075	3.709
T2	2.163	2.156	-0.007	-0.324
T3	2.056	---	---	---
T4	2.145	2.256	0.111	5.175
T5	2.056	2.210	0.154	7.490
T6	2.075	2.123	0.048	2.313
T7	2.012	2.064	0.052	2.584
T8	2.062	2.138	0.076	3.686
T9	2.120	2.135	0.015	0.708
T10	1.956	2.167	0.211	10.787
avg	2.0632	2.1054	0.0422	2.1068
sd	0.0843	0.0812	0.0675	3.3373
COV(%)	4.0881	3.8551		

paired t-test statistic = 3.367

=====

AITC Project 8704R: Phase II Douglas-fir Glulam Beams

=====

E/G = 16
Using Equation 5.2 for the E-transformation

Beam ID	Actual E (Mpsi)	Pred E (Mpsi)	diff (Mpsi)	error (%)
B1	2.143	2.113	-0.030	-1.400
B2	1.943	1.979	0.036	1.853
B3	1.958	1.984	0.026	1.328
B4	2.085	2.054	-0.031	-1.487
B5	2.214	2.170	-0.046	-2.076
B6	2.136	2.070	-0.066	-3.090
B7	2.034	2.026	-0.008	-0.393
B8	2.094	2.031	-0.063	-3.009
B9	2.127	2.104	-0.023	-1.081
B10	2.072	2.035	-0.037	-1.786
R1	1.984	1.993	0.089	4.674
R2	2.072	2.139	0.067	3.234
R3	2.056	2.196	0.140	6.809
R4	2.105	2.114	0.009	0.428
R5	2.082	2.174	0.092	4.419
R6	1.843	1.960	0.117	6.348
R7	2.054	2.044	-0.010	-0.487
R8	2.057	2.063	0.006	0.292
R9	2.203	2.249	0.046	2.088
R10	2.038	2.070	0.032	1.570
T1	2.022	2.091	0.069	3.412
T2	2.163	2.143	-0.020	-0.925
T3	2.056	---	---	---
T4	2.145	2.237	0.092	4.289
T5	2.056	2.195	0.139	6.761
T6	2.075	2.114	0.039	1.880
T7	2.012	2.057	0.045	2.237
T8	2.062	2.126	0.064	3.104
T9	2.120	2.125	0.005	0.236
T10	1.956	2.156	0.200	10.225
=====				
avg	2.0632	2.0970	0.0338	1.7053
sd	0.0843	0.0760	0.0658	3.2605
COV(X)	4.0881	3.6236		

paired t-test statistic = 2.762

=====

AITC Project 8704R: Phase II Douglas-fir Glulam Beams

=====

E/G = 20 for all lams except L3 where E/G = 30
 Using Equation 5.2 for the E-transformation

Beam ID	Actual E (Mpsi)	Pred E (Mpsi)	diff (Mpsi)	error (%)
B1	2.143	2.036	-0.107	-4.993
B2	1.943	1.911	-0.032	-1.647
B3	1.958	1.917	-0.041	-2.094
B4	2.085	1.983	-0.102	-4.892
B5	2.216	2.091	-0.125	-5.641
B6	2.136	1.998	-0.138	-6.461
B7	2.034	1.955	-0.079	-3.884
B8	2.094	1.959	-0.135	-6.447
B9	2.127	2.029	-0.098	-4.607
B10	2.072	1.965	-0.107	-5.164
R1	1.904	1.925	0.021	1.103
R2	2.072	2.062	-0.010	-0.483
R3	2.056	2.114	0.058	2.821
R4	2.105	2.037	-0.068	-3.230
R5	2.082	2.095	0.013	0.624
R6	1.843	1.895	0.052	2.821
R7	2.054	1.973	-0.081	-3.944
R8	2.057	1.992	-0.065	-3.160
R9	2.203	2.165	-0.038	-1.725
R10	2.038	1.998	-0.040	-1.963
T1	2.022	2.016	-0.006	-0.297
T2	2.163	2.066	-0.097	-4.485
T3	2.056	---	---	---
T4	2.145	2.154	0.009	0.420
T5	2.056	2.114	0.058	2.821
T6	2.075	2.038	-0.037	-1.783
T7	2.012	1.986	-0.026	-1.292
T8	2.062	2.050	-0.012	-0.582
T9	2.120	2.049	-0.071	-3.349
T10	1.956	2.078	0.122	6.237
=====				
avg	2.0632	2.0224	-0.0408	-1.9060
sd	0.0843	0.0711	0.0646	3.1220
COV(%)	4.0881	3.5174		

paired t-test statistic = -3.398

APPENDIX F**COMPARISON OF LOCALIZED SHEAR-FREE E AND LONG-SPAN E**

OVERVIEW OF EXPERIMENTAL DESIGN

Lumber was sampled in the summer of 1991 from one laminator located in the Pacific northwest United States. This laminator supplied 32 pieces of 16 ft. 2 x 6 Douglas fir lumber visually graded as L1. The lumber was selected by regrading machine stress rated (MSR) laminating lumber. If the lumber qualified for L1, every fifth piece was selected until 32 pieces had been collected.

The following information was recorded for each of the 32 pieces: moisture content, dimension, short-span modulus of elasticity (E_s) on 5 adjacent two-ft long segments and long-span modulus of elasticity E_{1S} .

TESTING EQUIPMENT

Two-ft Modulus of Elasticity Equipment

All specimens were nondestructively tested in bending to determine E_s . The bending test machine used was originally designed and fabricated for Taylor's (1988) localized lumber properties research. This equipment performs a bending test using "third-point" loading conditions. Third-point loading is defined as a static bending test with two equal and symmetrically placed loads applied to a simply supported test specimen. The theoretical shear-free, flatwise bending E , between the loads, was calculated from the force and deflection data collected during the testing procedure.

A computerized data acquisition and control system was also used that was designed for Taylor's (1988) research. This system allows continuous measurement of the force exerted on the test specimen and the relative deflection between the two load heads.

The load was measured by a load cell mounted between the hydraulic ram and the test frame to an accuracy of ± 0.1 lbs. The deflection was measured using a linear variable

displacement transducer (LVDT) mounted to the middle of the load head mechanism. This LVDT measured the relative deflection between the two loads for the test specimen. The deflection data was recorded to an accuracy of ± 0.001 in.

The signals from the load cell and the LVDT were connected to a data acquisition system (DAS) installed in a Compaq Portable II computer. These data later were used to calculate E_g . The DAS also automatically controlled the hydraulic operation and retracted the load head at a predetermined load.

Long-Span Modulus of Elasticity Equipment

All of the test specimens were subjected to another nondestructive bending test to determine long-span E . Long-span E is based on a static, flatwise bending test with a simply supported center point concentrated load and a span-to-depth (L/d) ratio of approximately 100 to minimize the effects of shear deflection. The reactions provide unrestrained support at both ends of the test specimen; however, the support at one end was allowed to tilt to match the twist of the lumber. Preload and final weights of 8.80 and 51.10 lbs were used.

TESTING PROCEDURE

The lumber was assigned identification numbers at the laminator's plant then the test specimens were shipped to the Agricultural Engineering Research Laboratory at Texas A&M University where all tests were conducted. All test were performed in accordance with AITC T116 Modulus of Elasticity of E-Rated Lumber by Static Loading (AITC, 1990), ASTM D198 Standard Methods of Static Tests of Timbers in Structural Sizes (ASTM, 1991a) and ASTM D4761 Standard Test Methods for Mechanical Properties of Lumber and Wood-Based Structural Material (ASTM, 1991f).

The lumber was "stickered" to allow it to condition to an equilibrium moisture content of approximately 12%. The moisture content was measured with a resistance-type moisture meter. These measurements then were converted to dry-basis moisture content using calibration data from oven tests. Moisture content was measured in three locations: midspan and 36 in. from each end. The moisture meter readings were measured to the nearest 0.1% (wet-basis).

Five two-ft segments were marked and numbered for each test specimen. The dimensions of each specimen were measured at approximately the same location the moisture samples were collected. The dimensions were measured using digital calipers. The thickness was measured to the nearest 0.001 in. and the width was rounded to the nearest 0.01 in. This was required because E is more sensitive to errors in thickness than it is to width measurements.

Each specimen was tested in flatwise bending to determine E_s at the five segments. These measurements were repeated for both sides of the specimens. The theoretical shear-free E between the load heads was determined by the following equation. This equation is valid only for "third point" loading.

$$E_s = \frac{P}{\Delta_R} \frac{L^3}{36 bh^3} \quad (F.1)$$

where:

- E_s = two-ft static bending modulus of elasticity,
- P = total concentrated load on specimen,
- Δ_R = deflection of the neutral axis of the beam relative to the load heads,
- L = total test span of the specimen,
- b = width of the specimen and
- h = thickness of the specimen.

The short-span bending test used a span of 6 ft. with a distance between load heads of 2 ft. Force and deflection data were sampled by the DAS at a rate of 5 Hz between the

range of 150 lbs and 400 lbs. Linear regression was used to determine the P/Δ_r term. The average dimensions for the lumber were substituted for b and h .

The long-span E was measured for all specimens on both sides. The long-span E is calculated by the following equation.

$$E_{LS} = \frac{P}{\Delta_T} \frac{L^3}{4bh^3} \quad (F.2)$$

where:

- E_{LS} = long-span static bending modulus of elasticity and
 Δ_T = total midspan deflection.

The long-span bending test used a span of 12.5 ft. Deflection data was measured manually with a dial indicator to the accuracy of 0.001 in. A preload of 8.80 lbs was applied at midspan and the deflection was measured underneath the load. A final load of 51.10 lbs was then placed at midspan and the total deflection was recorded instantly to minimize the result of load creep. The difference between the two deflections was substituted for Δ_T and P was equal to the difference between the final load and the preload (42.30 lbs).

EXPERIMENTAL RESULTS

The lumber was allowed to condition to its equilibrium moisture content inside a controlled environment. The average dry-basis moisture content for the sample was 11.77% with a standard deviation of 0.59% at the time testing began. The width and thickness were measured for the sample. The average width and standard deviation was 5.504 in. and 0.009 in., respectively. The thickness averaged 1.502 with a standard deviation of 0.002 in. The average of the five two-ft modulus of elasticities were compared to the long-span E measurements. Table F.1 contains the data from testing side-A and Table F.2 contains data from testing side-B.

Table F.1: Comparison of localized shear-free E and long-span E - Side-A

Board ID number	Modulus of Elasticity					avg*	L-span†	
	seg 1	seg 2	seg 3	seg 4	seg 5			
1	3.127	3.268	3.227	3.163	3.170	3.191	2.99	
2	2.831	2.511	2.537	2.535	2.488	2.581	2.32	
3	2.213	2.177	2.441	2.254	2.158	2.248	2.18	
4	2.226	2.130	2.082	2.012	1.946	2.079	1.93	
5	1.780	1.793	1.886	1.855	1.850	1.833	1.82	
6	1.837	1.896	1.841	1.870	1.735	1.836	1.79	
7	2.164	2.233	2.254	2.248	2.208	2.221	2.19	
8	1.777	1.821	1.884	1.799	1.755	1.807	1.80	
9	2.248	2.261	2.292	2.174	2.221	2.239	2.16	
10	2.036	2.192	2.186	2.363	2.488	2.253	2.14	
11	2.639	2.708	2.573	2.840	2.824	2.717	2.42	
12	1.331	1.503	1.480	1.417	1.459	1.438	1.47	
13	1.683	1.798	1.790	1.767	1.728	1.753	1.76	
14	2.406	2.485	2.459	2.546	2.608	2.501	2.31	
15	2.108	2.219	2.346	2.236	2.430	2.268	2.15	
16	2.632	2.634	2.566	2.687	2.774	2.659	2.44	
17	2.801	2.860	2.832	2.711	2.533	2.748	2.63	
18	1.842	1.978	1.875	2.049	2.061	1.961	1.95	
19	1.817	1.778	1.782	1.775	1.809	1.793	1.80	
20	2.347	2.531	2.591	2.547	2.446	2.492	2.39	
21	2.669	2.674	2.487	2.169	2.252	2.450	2.31	
22	2.521	2.277	2.592	2.625	2.526	2.508	2.34	
23	1.843	1.939	2.062	2.145	2.166	2.031	1.08	
24	2.908	2.812	2.827	2.853	2.706	2.821	2.71	
25	2.518	2.572	2.385	2.247	2.188	2.382	2.36	
26	1.610	1.795	1.886	1.895	2.020	1.841	1.82	
27	2.183	2.193	2.128	2.035	1.892	2.087	1.99	
28	1.545	1.630	1.709	1.826	1.872	1.716	1.70	
29	1.931	1.910	1.880	1.901	1.820	1.888	1.86	
30	1.993	1.909	1.935	1.979	1.927	1.948	1.91	
31	1.441	1.381	1.336	1.376	1.378	1.383	1.38	
32	1.772	1.823	1.700	1.674	1.724	1.739	1.72	
						avg	2.1691	2.0565
						sd	0.4276 [‡]	0.3982
						COV(%)	19.71	19.36

* Average of the five 2-ft segments

† Long-span E measured at a L/d ratio of 100

‡ Sample standard deviation of all 2-ft segments

Table F.2: Comparison of localized shear-free E and long-span E - Side-B

Board ID number	Modulus of Elasticity					avg [*]	L-span [†]
	seg 1	seg 2	seg 3	seg 4	seg 5		
1	3.028	3.141	3.194	3.210	3.228	3.160	2.98
2	2.562	2.367	2.385	2.353	2.329	2.399	2.31
3	2.137	2.106	2.366	2.203	2.192	2.201	2.17
4	2.059	1.992	1.945	1.901	1.824	1.944	1.92
5	1.831	1.915	2.035	1.893	1.832	1.901	1.81
6	1.808	1.867	1.809	1.837	1.735	1.811	1.79
7	2.145	2.197	2.271	2.184	2.140	2.187	2.17
8	1.802	1.796	1.862	1.796	1.768	1.805	1.80
9	2.230	2.250	2.288	2.159	2.203	2.226	2.18
10	1.998	2.117	2.088	2.291	2.436	2.186	2.13
11	2.700	2.705	2.615	2.913	2.917	2.770	2.45
12	1.397	1.507	1.471	1.481	1.584	1.488	1.45
13	1.650	1.731	1.762	1.749	1.733	1.725	1.78
14	2.415	2.488	2.418	2.493	2.616	2.486	2.34
15	2.008	2.125	2.206	2.137	2.339	2.163	2.13
16	2.470	2.521	2.515	2.567	2.566	2.528	2.46
17	2.708	2.815	2.865	2.783	2.640	2.762	2.64
18	1.916	2.049	1.899	2.104	2.122	2.018	1.95
19	1.823	1.789	1.772	1.762	1.799	1.789	1.81
20	2.276	2.436	2.474	2.562	2.529	2.455	2.37
21	2.605	2.591	2.406	2.140	2.230	2.394	2.31
22	2.391	2.186	2.463	2.493	2.425	2.392	2.32
23	2.094	2.025	2.136	2.422	2.308	2.197	2.01
24	2.877	2.848	2.847	2.819	2.670	2.812	2.71
25	2.535	2.736	2.520	2.332	2.272	2.479	2.36
26	1.664	1.850	1.930	1.973	2.042	1.892	1.83
27	2.147	2.194	2.098	2.000	1.840	2.056	2.00
28	1.525	1.613	1.695	1.761	1.825	1.684	1.70
29	1.975	1.940	1.909	1.943	1.837	1.921	1.85
30	2.104	2.023	1.945	1.979	2.003	2.011	1.91
31	1.431	1.389	1.317	1.386	1.368	1.378	1.37
32	1.809	1.838	1.782	1.685	1.769	1.777	1.72
					avg	2.1562	2.0851
					sd	0.4103 [‡]	0.3592
					COV(%)	19.03	17.23

* Average of the five 2-ft segments

† Long-span E measured at a L/d ratio of 100

‡ Sample standard deviation of all 2-ft segments

An interesting point should be noted about the data. The ratio of E_{LS} to the average E_S is 0.96. This is very similar to Taylor's (1988) findings. Taylor found the ratio to be 0.95 and 0.96 for 302-24 and L1 lumber grades, respectively.

There was little difference between the sides being tested; therefore, all data were grouped together for a regression analysis excluding one side of one specimen that had an extremely low long-span E and was considered an outlier; therefore, the sample size was equal to 63. Figure F.1 illustrates the plot of E_S versus E_{LS} .

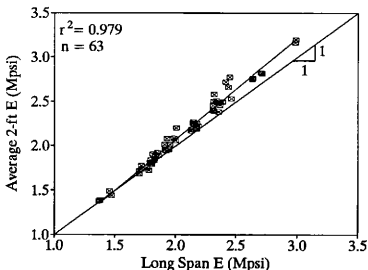


Figure F.1: E_S versus E_{LS} test data.

The regression equation relating these two values was found as:

$$E_S = 1.142 * E_{LS} - 0.219 \quad (F.3)$$

An interesting point about Equation F.3 should be noted. Kline et al. (1986) did a similar experiment except their short-span segments were 30 in. instead of 24 in. Their data indicate that the average of the E_S is close to E_{LS} (no more than 0.63% difference);

however using the regression equation developed from this research, any E_{1S} greater than 1.54 Mpsi yield an average E_8 that is greater than E_{1S} . This indicates the average two-ft E is higher than the long-span E for practically the whole data set of L1 laminating lumber. It is believed that a possible source of error could be caused by a crushing from the load heads for the 2-ft E measurements. A specimen with two million psi E would only take 0.006 in. of crushing to cause a 5% error in the measurement. To put this localized crushing in perspective, 0.006 in. is about 1.5 times greater than the thickness of a piece of paper. This is one possible explanation for the experimental error. This experimental error is significant because AITC has adopted this procedure for collecting lumber property data.

SUMMARY

Data were collected on 32 pieces of 16 ft. 2 x 6 Douglas-fir laminating lumber. The lumber was subjected to several nondestructive test including E_8 and E_{1S} . The test data indicate that the average E_8 value collected during this research does not equal E_{1S} which is counterintuitive.

VITA

Thomas D. Skaggs was born in Amarillo, Texas on August 10, 1967; son of Grady and Nancy Skaggs. He attended high school in his rural agricultural community. During his years at Adrian High School he was active in several organizations including 4-H and Future Farmers of America (FFA). He was president of both local clubs and was a district officer in FFA.

He pursued his agricultural interest by attending his father's alma mater, Texas A&M University. Tom finished his undergraduate degree in Agricultural Engineering in December of 1989. Immediately after graduation he stayed in the Agricultural Engineering Department to work toward his Master of Science Degree.

During Tom's tenure at Texas A&M, he was an active member of the Fraternity of Phi Gamma Delta. Honor societies include: Tau Beta Pi, Alpha Epsilon, Gamma Sigma Delta and Alpha Zeta.

Upon completion of his M.S. Degree, Tom chose to pursue his academic career by working toward his Doctor of Philosophy at Virginia Polytechnic Institute and State University (Va. Tech) in Blacksburg, Virginia.

His permanent address is:

c/o Grady S. Skaggs
P.O Box 37
Adrian, TX 79001